

Final Report  
(CSM Project 4-42163)

Joint Research Program between MMS and Pemex/IMP Underwater  
Wet Welding for Offshore Structures and Pipelines in the Gulf of  
Mexico: Process Maturation and Technology Transfer

Submitted to:  
Mr. Michael Else  
Minerals Management Service  
Engineering and Research Branch  
381 Elden St. Herndon, VA 20170  
And  
Instituto Mexicano del Petroleo  
Eje Central Lazaro Cardenas No. 152  
Mexico City, 07734

Prepared by:  
Stephen Liu and Faustino Perez Guerrero  
Center for Welding, Joining and Coatings Research  
Colorado School of Mines  
Golden, Colorado 80401  
CSM Report #: MT-CWJCR-004-025

Research Performed Under Contract:  
0101PO18117

August 2004

## TABLE OF CONTENTS

	Page
Executive summary.....	1
1. Introduction.....	3
1.1 Background.....	3
1.2 Objective.....	3
1.3 Organization of the report.....	3
2. Experimental procedure.....	4
2.1 Participants.....	4
2.2 Experimental setup.....	4
2.3 Steels and welding consumables.....	6
2.4 Initial wet welds.....	9
2.5 Bead-on-plate wet welds.....	9
2.6 Multipass V-groove type welds.....	10
2.7 Mechanical testing.....	10
2.7.1 Tensile testing.....	11
2.7.2 Charpy impact testing.....	11
2.7.3 Bend testing.....	12
3. Results.....	13
3.1 Initial bead-on-plate wet welds.....	13
3.2 Bead-on-plate wet welds.....	15
3.2.1 On ASTM A36 steel.....	16
3.2.2 On ASTM A572 Gr. 50 steel.....	23
3.2.3 On API 5L Gr. B steel.....	26
3.3 Multipass V-groove wet welds.....	29
3.3.1 On ASTM A36 Steel.....	30
3.3.2 On ASTM A572 Gr. 50 steel.....	31
3.3.3 On API 5L Gr. B steel.....	31
3.3.4 Porosity of the V-groove wet welds.....	31
3.4 Mechanical testing.....	35
3.4.1 Tensile Testing.....	35
3.4.2 Charpy impact testing.....	37
3.4.3 Bend testing.....	38
4. Conclusions and Recommendations.....	41
4.1 Conclusions.....	41
4.2 Recommendations.....	42
5. Acknowledgments.....	44

## List of Tables

Table 1. Chemical composition of the steels used to deposit the wet welds.....	6
Table 2. Welding current used to deposit bead-on-plate wet welds with the three electrodes at two water depths.....	9
Table 3. Welding current values to deposit bead-on-plate wet welds with three electrodes on three steels at two water depths.....	9
Table 4. Specimens extracted from the V-groove wet welds.....	11
Table 5. Performance of the three electrode types at two water depths.....	13
Table 6. Averaged bead morphology values of the bead-on-plate wet welds deposited with the three electrodes at two water depths on A36 steel.....	17
Table 7. Width and penetration measured on three cross-sections of the bead-on-plate wet weld deposited with E6013 electrode at 50 m and electrode negative.....	18
Table 8. Averaged porosity percentages measured on the cross-sections of the bead-on-plate wet welds deposited with the three electrodes at two water depths on A36 steel plates.....	18
Table 9. Metal transfer modes in wet welds deposited on A36 steel.....	21
Table 10. Mean voltage, current, welding speed, and heat input values calculated from the acquired arc signals from the BOP wet welds deposited on A36 steel.....	22
Table 11. Averaged bead morphology values of the bead-on-plate wet welds deposited with the three electrodes at two water depths on A572 Gr. 50 steel.....	23
Table 12. Averaged porosity percentages measured on the cross-sections of the bead-on-plate wet welds deposited with the three electrodes at two water depths on A572 Gr. 50 steel plates.....	24
Table 13. Metal transfer modes in wet welds deposited on A572 Gr. 50 steel.....	25
Table 14. Mean voltage, current, welding speed, and heat input values calculated from the acquired arc signals from the BOP wet welds deposited on A572 Gr. 50 steel.....	25
Table 15. Averaged bead morphology values of the bead-on-plate wet welds deposited with the three electrodes at two water depths on API 5L GR. B steel.....	26
Table 16. Averaged porosity percentages measured on the cross-section of the bead-on-plate wet welds deposited with the three electrodes at two water depths on API 5L Gr. B steel plates.....	27
Table 17. Metal transfer modes in wet welds deposited on API 5L Gr. B steel.....	28
Table 18. Mean voltage, current, welding speed, and heat input values calculated from the acquired arc signals from the BOP wet welds deposited on API 5L Gr. B steel.....	28
Table 19. Tensile test results of wet welds deposited at 50 m.....	35
Table 20. Tensile test results of wet welds deposited at 100 m.....	35
Table 21. Charpy impact test results of wet welds deposited at 50 m.....	37
Table 22. Charpy impact test results of wet welds deposited at 100 m.....	37
Table 23. Side bend test results of wet welds deposited at 50 m.....	39
Table 24. Side bend test results of wet welds deposited at 100 m.....	39

## List of Figures

Figure 1. (a) Hyperbaric chamber used to perform the wet welds and (b) gravity welder inside the chamber. ....	4
Figure 2. (a) Gravity welder and (b) depositing a dry weld with the gravity welder. ....	5
Figure 3. Steel coupons prepared to deposit the bead-on-plate wet welds, the dimensions shown are in mm (1/2"x 4" x10"). ....	7
Figure 4. Steel coupons prepared for the multipass V-groove wet welds, the dimensions shown are in mm (1/2"x3.1"x10"). ....	7
Figure 5. Commercial electrodes used to deposit the wet welds AWS E7024, E7018 and E6013 from left to right hand side. The electrode flux coating thickness is 3.0 mm for the E7024, 1.5 mm for the E7018, and 1 mm for the E6013. ....	8
Figure 6. Location and orientation of specimens for mechanical testing extracted from the multipass V-groove wet welds. ....	10
Figure 7. Dimensions of the specimens for tensile testing (dimensions in millimeters). ....	11
Figure 8. Dimensions of the Charpy V-notch specimens (a) plan view and (b) transverse cross-section (dimensions in millimeters). ....	12
Figure 9. Dimensions of side bend specimens (dimensions in millimeters). ....	12
Figure 10. Photographs of the initial bead-on-plate wet welds deposited with the three electrodes with different current values at 100 m. ....	14
Figure 11. Transverse cross-sections from BOP wet welds deposited with E7018 electrode at 100 m, the welding current values used were 270, 290 and 310 A (from left to right hand side). ....	14
Figure 12. Cross-section macrographs of the initial bead-on-plate wet welds deposited with E6013 electrode type at 50 m using electrode positive. ....	15
Figure 13. (a) Location of the transverse cross-section extracted from the bead-on-plate wet welds and (b) bead-on-plate weld showing the width, depth or penetration, and reinforcement. ....	16
Figure 14. Photographs of the bead-on-plate wet welds deposited with the three electrode types using electrode positive (DCEP) on A36 steel plates at 50 m. ....	16
Figure 15. Cross-section macrographs from the center of the BOP wet welds deposited with the E6013, E7018 and E7024 electrodes using electrode positive (DCEP) at 50 m (scale in millimeters). ....	17
Figure 16. Microstructures of the bead-on-plate wet welds deposited with the three electrode types using electrode positive on A36 steel at 50 m. ....	19
Figure 17. Voltage signals recorded during wet welding with (a) E6013 electrode, (b) E7018 electrode, and (c) E7024 electrode on A36 steel at 50 m water depth. ....	21
Figure 18. Steel plate arrangement for V-groove welding. ....	29
Figure 19. V-groove wet weld inside the chamber after depositing another wet weld. ....	30
Figure 20. Cross-sections macrographs extracted (a) and (c) from the beginning and (b) and (d) from the end part of the V-groove welds. All four macrographs are shown at the same magnification. ....	32
Figure 21. X-ray radiographic image from the V-groove wet weld deposited with E7024 electrodes on API 5L Gr. B steel at 100 m. Larger pores are observed on the left hand side, which is the beginning of the weld. ....	33
Figure 22. Porosity versus water depth from V-groove wet welds deposited with E6013 electrodes on three steels. ....	33
Figure 23. Porosity versus water depth from V-groove wet welds deposited with E7024 electrodes on three steels. ....	34
Figure 24. Porosity versus steel type from V-groove wet welds deposited with E7024 and E6013 electrodes at 50 and 100 m. ....	34
Figure 25. Ultimate tensile strength of V-groove wet welds deposited with E6013 and E7024 electrode type at two water depths. ....	36
Figure 26. Charpy impact testing results of reduced size specimens machined from the V-groove wet welds, the tests were carried out at a temperature of 32 °F (0 °C). ....	38
Figure 27. Results from the side bend test (a) specimens extracted from V-groove welds deposited with E6013 electrode and (b) with E7024 electrode. ....	40

## **Appendices**

### Appendix A - Analysis of the arc signals acquired during wet welding

- A.1 Arc voltage signals
- A.2 Arc voltage signals with direct current electrode positive (DCEP)
  - A.2.1 BOP welds on A36 Steel
  - A.2.2 BOP welds on A572 Gr. 50 Steel
  - A.2.3 BOP welds on API 5L Gr. B steel
- A.3 Arc voltage signals with direct current electrode negative (DCEN)
  - A.3.1 BOP welds on A36 steel
  - A.3.2 BOP welds on A572 Gr. 50 steel
  - A.3.3 BOP welds on API 5L Gr. B steel
- A.4 Arc current signals with direct current electrode positive (DCEP)
  - A.4.1 BOP welds on A36 steel
  - A.4.2 BOP welds on A572 Gr. 50 steel
  - A.4.3 BOP welds on API 5L Gr. B steel
- A.5 Arc current signals with direct current electrode negative (DCEN)
  - A.5.1 BOP welds on A36 steel
  - A.5.2 BOP welds on A572 Gr. 50 steel
  - A.5.3 BOP welds on API 5L Gr. B steel
- A.6 Summary of results

### Appendix B - Bead-on-plate wet welds

- B.1 Initial bead-on-plates wet welds
- B.2 Bead-on-plate wet welds
  - B.2.1 BOP welds on A36 Steel
  - B.2.2 BOP welds on A572 Gr. 50 Steel
  - B.2.3 BOP welds on API 5L Gr. B steel

### Appendix C - Cross-section macrographs from the bead-on-plate wet welds

- C.1 Initial bead-on-plate wet welds
- C.2 Bead-on-plate wet welds
  - C.2.1 BOP welds on A36 Steel
  - C.2.2 BOP welds on A572 Gr. 50 Steel
  - C.2.3 BOP welds on API 5L Gr. B steel

### Appendix D - Microstructures of the Bead-on-plate wet welds

D.1 Microstructures of the bead-on-plate wet welds

D.1.1 BOP welds on A36 Steel

D.1.2 BOP welds on A572 Gr. 50 Steel

D.1.3 BOP welds on API 5L Gr. B steel

Appendix E - Photographs and X-ray radiographs of the V-groove wet welds

E.1 Photographs and X-ray radiographs of the V-groove wet welds

E.1.1 On A36 Steel

E.1.2 On A572 Gr. 50 Steel

E.1.3 On API 5L Gr. B steel

Appendix F - Cross-section macrographs of the V-groove wet welds

F.1 Porosity on cross-section macrographs of the V-groove wet welds

F.1.1 On A36 Steel

F.1.2 On A572 Gr. 50 Steel

F.1.3 On API 5L Gr. B steel



## EXECUTIVE SUMMARY

Three commercial electrodes (AWS E6013, AWS E7018 and AWS E7024) have been tested in fresh water at two simulated water depths (50 and 100 m). Three typical steels used in the fabrication of aging offshore structures have been selected to deposit the wet welds. Bead-on-plate (BOP) and V-groove wet welds have been deposited on the three steels at two water depths. The wet welds have been deposited inside a hyperbaric chamber using a gravity welding system. A special conductive paste made with fluxes has been designed and successfully used to start the arc of the welds. One water depth (150 m) has not been considered in this research work due to technical difficulties to deposit the welds at this pressure, excessive porosity, poor bead morphologies, and arc instability. Instead detailed analyses of arc signals and direct current electrode negative have been added to the experimental matrix of the initial program.

One set of initial Bead-on-plate wet welds were deposited using different welding parameters in order to select the appropriate processing conditions to deposit the required wet welds. When the initial BOP welds were deposited, the performance of the arc was observed. Transverse cross-sections were extracted to correlate the welding parameters with the bead morphologies and porosity. Based on the results obtained with the initial BOP wet welds the welding parameters for each electrode and water depth were defined.

With the welding parameters defined, three BOP wet welds were deposited with each electrode grade on each steel type at the two water depths. Two BOP welds were made using electrode positive and the third weld with electrode negative. During welding, arc voltage and arc current signals were collected and recorded. Three transverse cross-sections were extracted from each BOP weld for bead morphology measurements, defects identification, metallographic analysis, and porosity measurement. From the results obtained, it was concluded that the E6013 electrode produced the lowest levels of porosity, followed by the E7024. E7018 electrodes produced excessive porosity. Large percentage of the pores in welds deposited with the E7024 electrode was localized on the topside of the weld beads; therefore it was considered that in multipass V-groove welds those pores close to the surface would be removed by subsequent weld passes. With regards to arc stability, the E7024 and E6013 electrodes performed satisfactorily in all cases. The E7018 electrode exhibited poor arc stability underwater, being arc extinction the main problem observed.

V-groove wet welds were made to extract specimens for mechanical testing. It was difficult to make V-groove welds using the E7018 electrodes due to the frequent arc extinctions. For the excessive porosity observed on the BOP welds and the arc instabilities during multipass V-groove welding, the E7018 electrode was considered unsuitable for wet welding applications. Porosity analysis on cross-sections from the V-groove wet welds showed that the E6013 electrode produced the lowest porosity level, thus exhibiting the highest mechanical properties than the welds deposited with the E7024 electrode.

Although the E7024 electrode type exhibited good performance underwater and the weld beads deposited presented good morphology, the porosity level observed is enough reason to limit its usage. The porosity is attributed to the thick flux covering, about three times

thicker than the flux coating in the E6013 electrode. Considering all factors, the E6013 electrode has demonstrated the best combined performance underwater.

In general the wet welds deposited with the AWS E6013 electrode grade meet or exceed the AWS D3.6M:1999 requirements for Class A welds. The welds deposited with the AWS E7024 electrode grade at 50 m meet the AWS D3.6M:1999 requirements for Class A welds.

# **1. INTRODUCTION**

## **1.1 Background**

Underwater wet welding offers an economical alternative for the repair of offshore structures in the oil industry, ships, and components in power plants. However, their use is mostly limited to secondary structural elements depending on the applicable codes due to defects and reduced mechanical properties. The loss of alloying elements during welding and porosity are the major factors in the reduced strength of the wet welds. However, the reduced strength could be overcome with proper measures such as over-designing the joint. Although various research projects have been carried out in this field, the conditions tested are not known therefore it is necessary to conduct research work under the interested conditions.

## **1.2 Objective**

The objective of this program is to study the performance of three commercial electrodes (E 6013, E7018 and E7024) in wet welding conditions on typical steels (A36, A572 Gr. 50 and API 5L Gr. B) used in the fabrication of aging offshore structures at three water depths (50, 100, and 150 m). Special attention is given to bead morphologies, welds defects, microstructures, steel chemical composition, porosity, and mechanical properties.

## **1.3 Organization of the report**

The report contains five sections starting with an executive summary, followed by an introduction in section 1, the experimental procedure is given in section 2, the obtained results are reported in section 3, the main conclusions and recommendations are presented in section 4, and the acknowledgments are presented in section 5. In order to support the results given in the report, six appendices were included. In Appendix A, the arc voltage and current signals acquired from the bead-on-plate wet welds are tabulated. Photographs of the bead-on-plate wet welds are provided in Appendix B. Cross-section macrographs from the bead-on-plate wet welds are presented in Appendix C. Appendix D contains micrographs that show the microstructures of the bead-on-plated wet welds, Appendix F presents photographs and X-ray radiographic images of the V-groove wet welds.

## 2. EXPERIMENTAL PROCEDURE

### 2.1 Participants

In order to achieve the goals of this project, it was necessary to subcontract an institution with the capabilities of depositing wet welds at three simulated water depths of 50, 100 and 150m. Among the institutions with such capabilities are GKSS, Germany, Global Divers Inc., U.S.A., and Federal University of Minas Gerais (UFMG), Belo Horizonte, Brazil. Based on availability, cost, and experience, UFMG was selected to carry out the experimental work.

The analysis and interpretation of the results were carried out at the Center for Welding, Joining and Coatings Research (CWJCR) at the Colorado School of Mines (CSM) with the collaboration of the Department of Mechanical Engineering at UFMG.

### 2.2 Experimental setup

A hyperbaric chamber designed for simulated water depths down to 200 m (656 ft) was used to deposit the required wet welds. Figure 1 shows the hyperbaric chamber at UFMG.

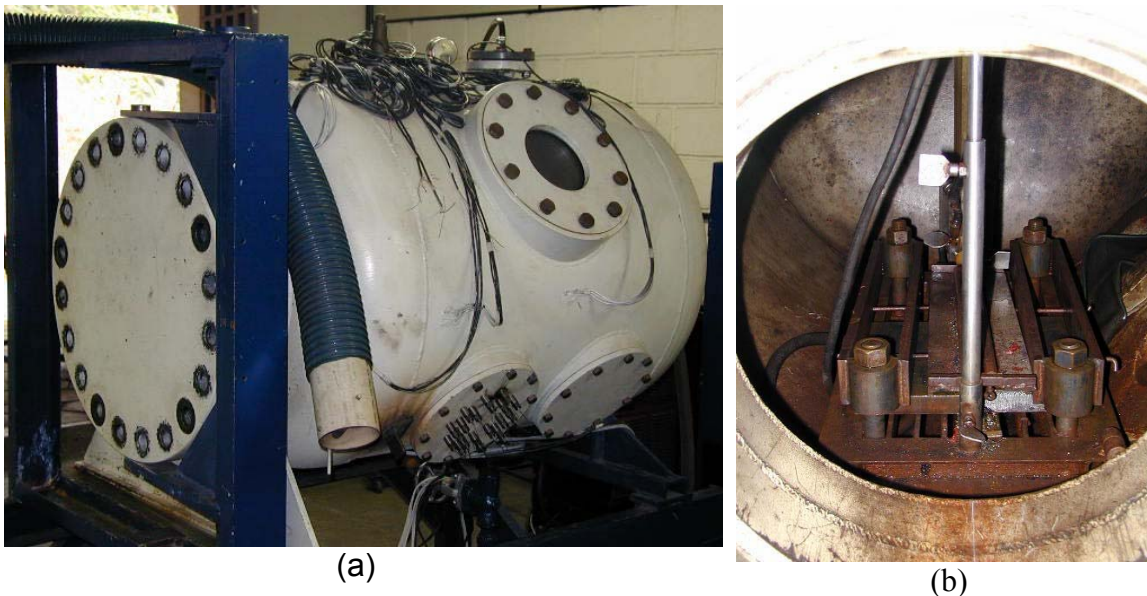


Figure 1. (a) Hyperbaric chamber used to perform the wet welds and (b) gravity welder inside the chamber.

There are three ways to deposit wet welds in a hyperbaric chamber, the first is manual, i.e. performed by a welder inside the chamber, the second is mechanical, with a gravity welding system, and the third is with an automated welding system. Manual welding has the advantage that more than one wet welds can be deposited per welding cycle. On the other hand, more equipment and personnel are required to decompress the welder at the right time intervals and to provide gas mixtures to avoid health damages. With the second

alternative the wet welds are deposited mechanically with a gravity welding system, thereby minimizing cost and simplifying the process. The disadvantages are that only one weld can be deposited per welding cycle and that if the arc does not start or extinguish before melting the whole electrode, the welding cycle has to be restarted. With the third option, the major advantage is that more than one weld could be deposited per welding cycle. The disadvantages are the requirement of special equipment inside the chamber and the need to waterproof the equipment. The second option was used to deposit the welds in this project.

The gravity welding system used is shown in Figure 2 (a), where one can see the electrode marked with letter *a*, the steel plate *b*, electrode holder *c*, and the sliding bar or guide of the electrode holder *d*. During welding, as the electrode melts the electrode holder slides down allowing the electrode tip to travel certain distance towards the sliding bar; this distance depends on the angle between the electrode and the steel plate (small electrode-plate angle results in a long weld, thus faster weld travel). Figure 2 (b) shows the gravity welder depositing a dry weld.

A Lincoln Power Wave 450 power source was used to deposit the wet welds with one power cable connected to the electrode holder and the other cable connected to the steel plate. Direct current electrode positive (DCEP) and direct current electrode negative (DCEN) polarities were used.

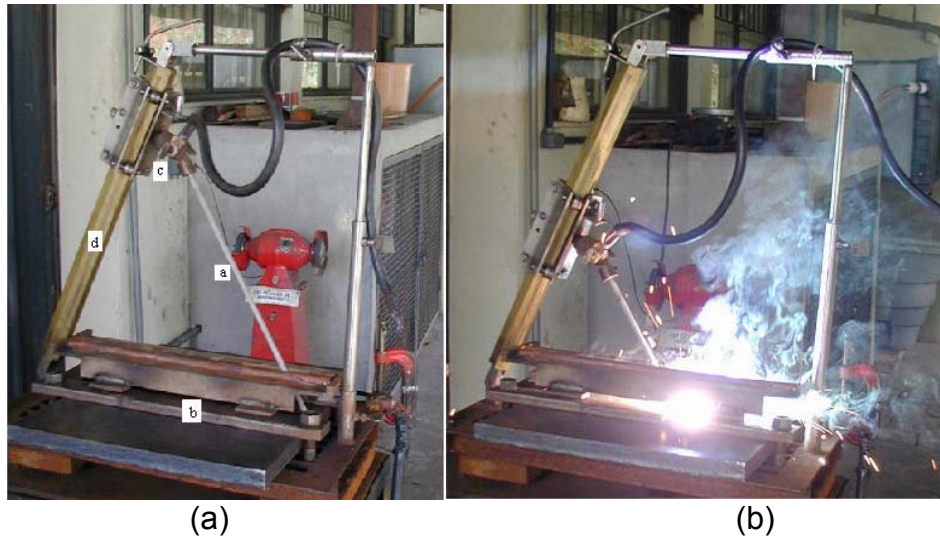


Figure 2. (a) Gravity welder and (b) depositing a dry weld with the gravity welder.

Once the welding parameters have been defined, a welding cycle in the pressure vessel using the gravity welder consists of the following steps:

- a) Place the steel plate and electrode in the gravity welder inside the chamber
- b) Close the chamber and tighten the nuts to the right torque
- c) Fill the chamber with fresh water

- d) Pressurize the chamber with compressed air to the desired pressure
- e) Start the arc
- f) Record arc signals
- g) Disconnect the power after arc extinguishes
- h) Release the air pressure
- i) Pump out the water
- j) Open the chamber
- k) Extract the welding fumes
- l) Remove the plate and clean the weld

Several welding cycles are needed to complete a multipass V-groove wet weld depending on the electrode diameter, V-groove angle, welding speed, pressure, steel plate thickness, and joint design.

Arc voltage and current signals were acquired from the power cables during welding, and digitalized and stored in a desktop computer. The arc signals were acquired at a rate of 250 data points per second.

### 2.3 Steels and welding consumables

Three steel plates typically used in aging offshore structures were used to deposit single bead-on-plate (BOP) and multipass V-groove wet welds. Table 1 presents the chemical composition of the three steels used.

Table 1. Chemical composition of the steels used to deposit the wet welds.

Steel	Element in wt. pct.											
	C	Si	Mn	P	S	Ni	Mo	V	Cu	Nb	Al	Ti
A36	0.14	0.22	0.76	0.014	0.009	0.010	0.0	0.003	0.008	0.002	0.030	0.008
A572 Gr. 50	0.12	0.14	0.70	0.017	0.007	0.0	0.0	0.002	0.005	0.0	0.007	0.008
API 5L Gr. B	0.15	0.19	1.37	0.014	0.008	0.007	0.003	0.003	0.009	0.020	0.008	0.018

Typically, carbon steels with carbon equivalent (CE) greater than 0.40 are difficult to weld, unless measures such as preheat or post-weld heat treatment are applied. The carbon equivalent for these steels was calculated with the equation recommended by the International Institute for Welding (IIW).

$$CE = C + \frac{Mn + Si}{6} + \frac{Ni + Cu}{15} + \frac{Cr + Mo + V}{5}$$

The CE values calculated for the A36, A572 Gr. 50, and API 5L Gr. B steel were 0.30, 0.26, and 0.41, respectively. Based on these results, some difficulties could be expected when wet welding the API 5L Gr. B steel which has the largest manganese content.

Small coupons were cut-off from the steel plates to deposit the BOP wet welds and V-groove multipass wet welds. Figure 3 and 4 illustrate the dimensions of the coupons used to deposit the BOP and V-groove wet welds, respectively.

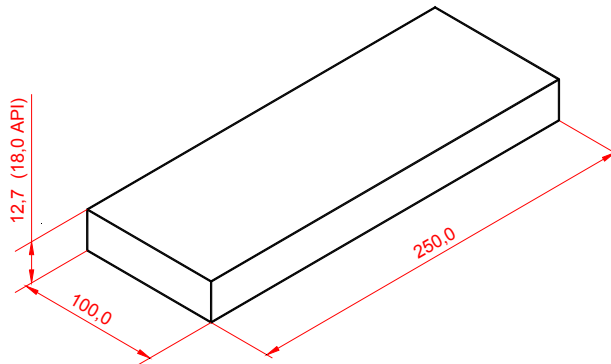


Figure 3. Steel coupons prepared to deposit the bead-on-plate wet welds, the dimensions shown are in mm (1/2"x 4" x10").

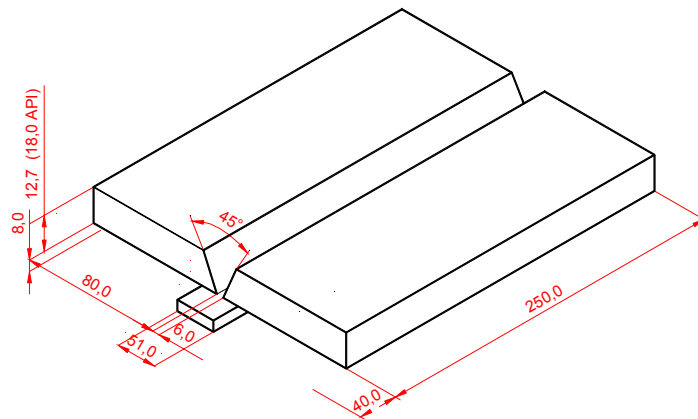


Figure 4. Steel coupons prepared for the multipass V-groove wet welds, the dimensions shown are in mm (1/2"x3.1"x10").

Three electrode types manufactured and commercialized by ESAB were used to deposit the wet welds. The first electrode type was the rutile grade AWS E6013 (OK 46.00), which is an all-position electrode with good bead appearance, recommended for all joint types in steel structures, and multiple applications. The second electrode was basic grade AWS E7018 (OK 48.06). This electrode is recommended for welding components or structures that require high quality weld metal with excellent impact resistance. The third electrode was also rutile grade AWS E7024 (OK 33.80), recommended for flat position. This electrode contains iron powder in the flux coating for high deposition rate.

The diameter of the steel rod of the three electrode types was 5.0 mm (3/16 in.). All electrodes measured 355 mm (14 in.) long. The thickness of the flux coating was 1, 1.5 and 3 mm for the E6013, E7018 and E7024 electrode type, respectively. Figure 5 shows the AWS E7024 (with thicker flux coating), AWS 7018, and AWS E6013 (from left to right.) Large diameter electrodes were selected because of their higher deposition rates. They can produce sizable weld beads requiring a smaller number of weld passes to complete the V-groove wet welds.



Figure 5. Commercial electrodes used to deposit the wet welds AWS E7024, E7018 and E6013 from left to right hand side. The electrode flux coating thickness is 3.0 mm for the E7024, 1.5 mm for the E7018, and 1 mm for the E6013

In order to protect the flux coating from moisture pickup the electrodes were hand coated with commercially available waterproofing varnish, followed by drying at room temperature for 24 hrs before welding. The varnished from the tip of the electrode is removed before placing each electrode in the gravity welder to have electrical contact with the conductive paste (described below) and the steel plate.

To start the arc without sticking the electrode on the plate, a special conductive paste was designed. The paste consists of iron-powder, iron-oxide powder, waterproofed glue, and sodium silicate. The ingredients are uniformly mixed and the paste rolled to a flat layer (1/4"), then dried at room temperature. The waterproofed glue gives flexibility to the paste and avoids dissolution of the mixture when submerged in water. A small section of paste is placed between the plate and the electrode tip making good electrical contact between the parts. When the welding setup is ready the electrical power flows through the cables and start the arc without short-circuiting the electrode on the plate.

## 2.4 Initial wet welds

In order to test the conductive paste designed to start the arc and to determine the right welding parameters for the three electrodes at two water depths, several BOP wet welds were deposited with each electrode type on A36 steel plates. The BOP welds were cross-sectioned to measure their porosity content. Table 2 presents the welding current values tested for each electrode at two water depths.

Table 2. Welding current used to deposit bead-on-plate wet welds with the three electrodes at two water depths.

Welding current used at 50 m, Amperes			Welding current used at 100 m, Amperes		
E6013	E7018	E7024	E6013	E7018	E7024
250	230	290	250	230	290
270	250	310	270	250	310
290	270	330	290	270	330
310	290	350	310	290	350
330	310	370	330	310	370
	330		350	330	390
	350				
	370				
	390				
	420				

## 2.5 Bead-on-plate wet welds

In addition to the initial BOP wet welds mentioned above, three BOP wet welds were deposited with each electrode type on the three steels and two water depths. Two BOP welds were made using DCEP and one BOP using DCEN polarity. The BOP wet welds were deposited with the gravity welder using the welding current values given in Table 3. The angle between the plate and the electrode was fixed at 60 degrees. The wet welds were cross-sectioned for bead morphology characterization, porosity measurement, and metallographic analysis.

Table 3. Welding current values to deposit bead-on-plate wet welds with three electrodes on three steels at two water depths.

Welding current used at 50 m, Amperes			Welding current used at 100 m, Amperes		
E6013	E7018	E7024	E6013	E7018	E7024
260	280	310	280	280	310

Signals from the arc (voltage and current) were recorded with a data acquisition system. A sampling frequency of 250 samples per second was used. The data collection started before

the arc started and ended after the arc extinguished. Therefore, the welding time can be known for each BOP wet weld from the recorded signals. The arc signals were analyzed to identify the metal transfer mode and arc stability for each electrode type at the two water depths.

**2.6 Multipass V-groove type welds**

Multipass V-groove wet welds were prepared with each electrode type on the three steels at two water depths. Figure 4 illustrate the plate dimensions and arrangement of these wet welds. In order to prepare specimens for mechanical testing it was necessary to deposit V-groove wet welds. The welds were deposited with the gravity welder using the welding current values given in Table 3. The angle between the plate and the electrode was fixed at 60 degrees. One side of the specimens machined for side bend testing was used for porosity measurement. Based on the difficulties to keep the arc open until the whole consumption of the electrode observed in the BOP and first V-groove weld, and based on the porosity level observed on the BOP welds, it was concluded that the E7018 electrode grade is not suitable for wet welding. Although the E7024 electrode grade exhibited more porosity than the E6013 electrode, high percentage of the pores were observed to be located on the topside of the beads. These pores can be removed with proper overlapping the next weld passes.

**2.7 Mechanical testing**

Mechanical testing was carried out on specimens extracted from the multipass V-groove wet welds deposited at two water depths with two electrodes on the three steels. Figure 6 illustrates the multipass V-groove wet weld showing location from where the specimens were extracted.

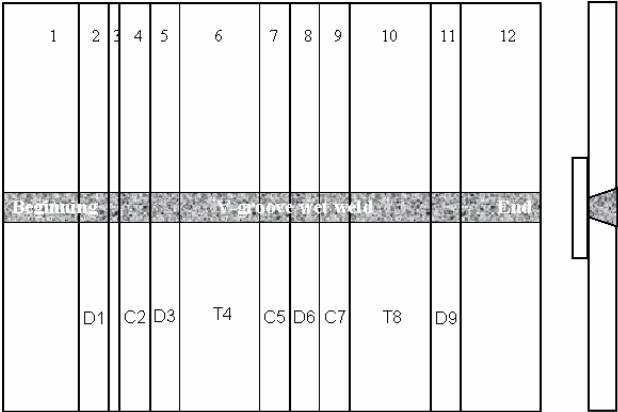


Figure 6. Location and orientation of specimens for mechanical testing extracted from the multipass V-groove wet welds.

The numbered areas shown in Figure 6 were used to machine specimens for mechanical testing as presented in Table 4.

Table 4. Specimens extracted from the V-groove wet welds.

Specimen	Use
1	Discarded
2	D1 Side bend specimen
3	Metallographic analysis
4	C2 Charpy specimen
5	D3 Side bend specimen
6	T4 Tensile specimen
7	C5 Charpy specimen
8	D6 Side bend specimen
9	C7 Charpy specimen
10	T8 Tensile specimen
11	D9 Side bend specimen
12	Discarded

### 2.7.1 Tensile Testing

Two flat tensile specimens (T4 and T8) were machined from each V-groove wet weld. The weld metal is located at the center of the specimen as illustrated in Figure 7.

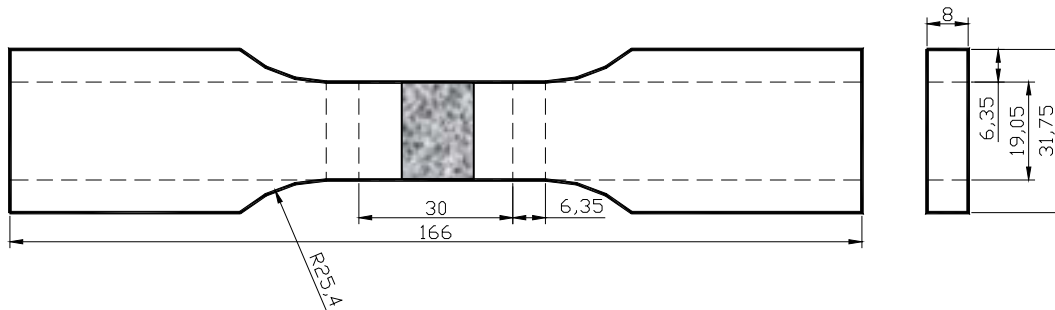


Figure 7. Dimensions of the specimens for tensile testing (dimensions in millimeters).

### 2.7.2 Charpy impact testing

Three reduced size Charpy V-notch specimens (C2, C5 and C7) were fabricated from each multipass wet weld. Figure 8 illustrates the dimensions of the specimens. The V-notch runs vertically through the different weld passes at the center of the V-groove welds.

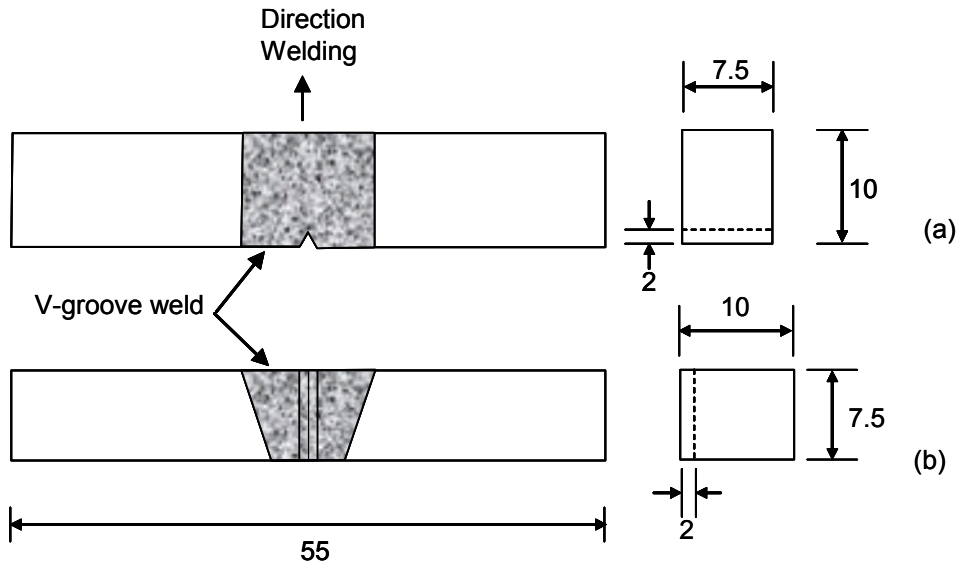


Figure 8. Dimensions of the Charpy V-notch specimens (a) plan view and (b) transverse cross-section (dimensions in millimeters).

### 2.7.3 Bend testing

Four specimens for side-bend testing (D1, D3, D6, and D9) were machined from each V-groove multipass weld; dimensions are shown in Figure 9.

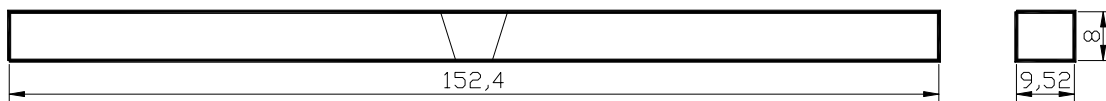


Figure 9. Dimensions of side bend specimens (dimensions in millimeters).

### 3. RESULTS

#### 3.1 Initial bead-on-plate wet welds

From the initial BOP wet welds deposited with the three electrode types on A36 steel, the performance of the electrodes was assessed. Table 5 presents the welding current values used, the number of attempts to start the arc, and arc extinction if present.

Table 5. Performance of the three electrode types at two water depths.

Electrode type	50 m water depth			100 m water depth		
	Selected welding current, Amperes	Number of attempts to start the arc	Arc extinction events	Selected welding current, Amperes	Number of Attempts to start the arc	Arc extinction events
E6013	250	2	No	250	2	No arc
	270	1	No	270	1	No
	290	1	No	290	1	No
	310	2	No	310	1	No
	330	2	No	330	1	Yes
				350	1	No
E7018	230	3	No	230	1	Yes
	250	2	Yes	250	1	No
	270	1	Yes	270	1	No
	290	3	Yes	290	1	No
	310	1	Yes	310	1	Yes
	330 *	2	Yes	330	1	Yes
	350 *	1	Yes			
	370 *	1	Yes			
	390 *	1	No			
420 *	1	Yes				
E7024	290	1	No	290	1	No
	310	1	No	310	1	No
	330	1	No	310	1	No
	350	1	No	330	1	No
	370	1	No	350	1	No
				370	1	No
			390	1	No	

\* Different angles between the electrode and steel plate were tested

With regards to the ability to start and maintain the arc until the full consumption of the electrode, Table 5 shows that E7024 electrode type presented the best performance, followed by the E6013. The E7018 had a poor performance because the arc extinguished frequently at the beginning of the welds.

Figure 10 shows photographs of the initial BOP wet welds deposited with the three electrodes on A36 steel, one can notice that the BOP welds deposited with E7024 electrode have similar lengths which means that the arc was maintained until the full electrode was consumed. On the other hand, less BOP welds were deposited with E7018 and each bead

was different in length indicating that the arc extinguished before melting the full electrode length. With the E6013 electrode only one BOP weld had slightly shorter length. Photographs of all the initial BOP wet welds are provided in Appendix B.

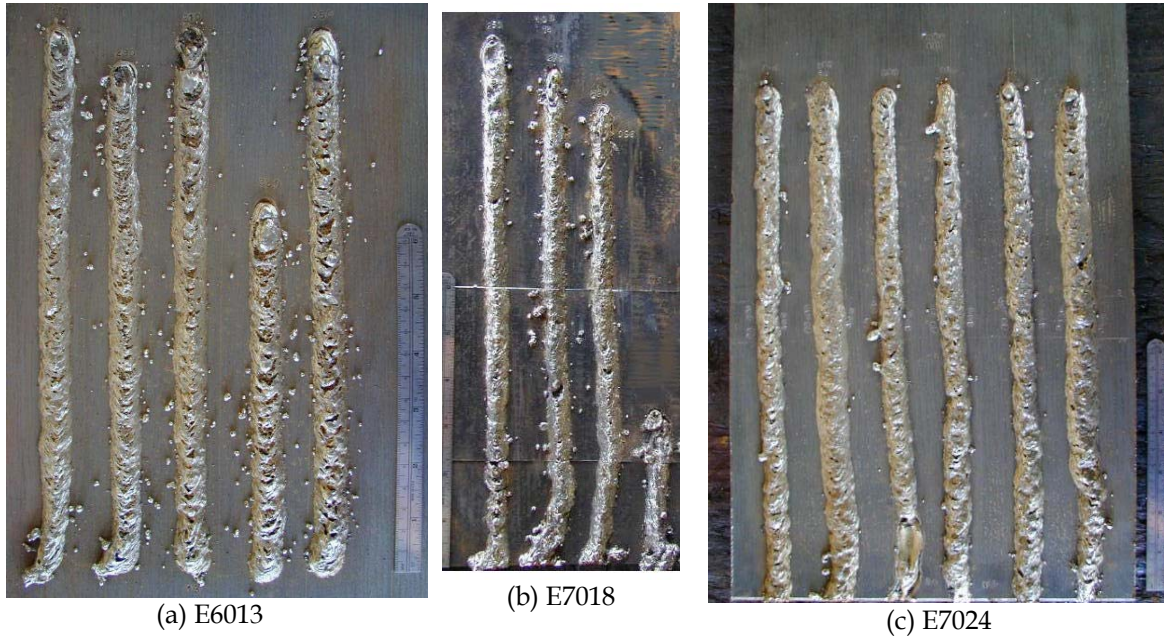


Figure 10. Photographs of the initial bead-on-plate wet welds deposited with the three electrodes with different current values at 100 m.

Figure 11 presents transverse cross-sections from a BOP wet weld deposited with E7018 electrode at 100 m. These macrographs show that porosity increases with increasing welding current values. For this reason, appropriate welding current values must be selected for each electrode type and each water depth. The severe porosity is a further indication that the E7018 flux design is not suitable for wet welding.



Figure 11. Transverse cross-sections from BOP wet welds deposited with E7018 electrode at 100 m, the welding current values used were 270, 290 and 310 A (from left to right hand side).

Transverse cross-section macrographs from BOP welds deposited at 50 m with E6013 electrode type using 250 and 270 A with DCEP show good bead morphologies and few pores, see Figure 12. Additional cross-section macrographs are given in Appendix C.

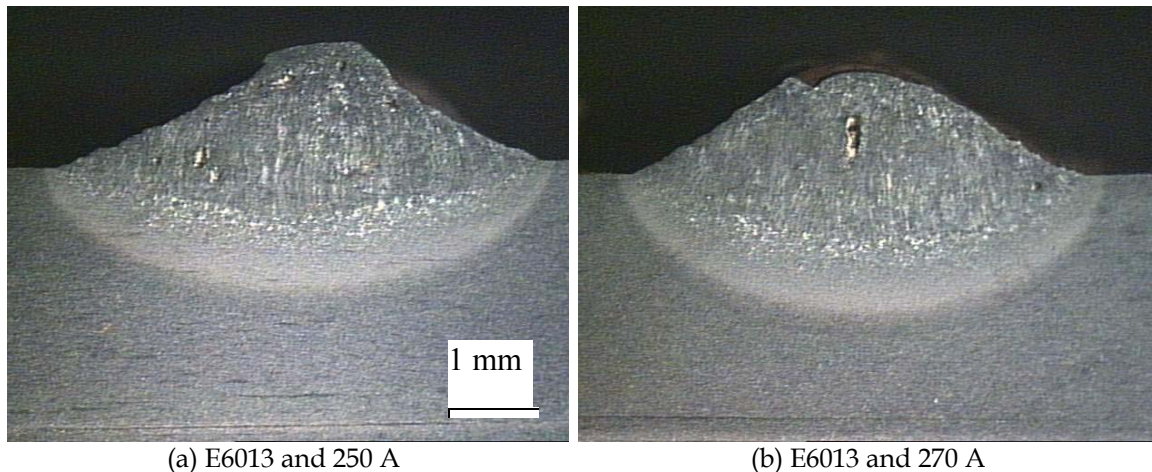


Figure 12. Cross-section macrographs of the initial bead-on-plate wet welds deposited with E6013 electrode type at 50 m using electrode positive.

From cross-section macrographs of the initial BOP wet welds it was determined that the best bead morphologies were the ones deposited with E6013 electrodes at 50 and 100 m. The welds made with the E7018 electrode show deeper penetration, higher reinforcement, and more porosity. Welds made with E7024 show better bead morphologies and less porosity than the ones made with E7018 electrode.

With this initial set of BOP wet welds the welding parameters were selected for each electrode type, as well as the procedure to conduct the BOP wet welds with the three electrodes on the three steels at two water depths and two polarities.

### 3.2 Bead-on-plate wet welds

The welding current values defined from the initial BOP wet welds given in Table 3 were used to deposit three BOP welds with each electrode type. Two BOP wet welds were deposited using DCEP, and one BOP using DCEN polarity. Three transverse cross-sections were extracted from the beginning, center, and end part of each weld, as illustrated in Figure 13 (a). The transverse cross-sections are provided in Appendix C. From the cross-section macrographs the bead morphologies (width, penetration under the plate surface, and the reinforcement) were characterized, as illustrated in Figure 13 (b).

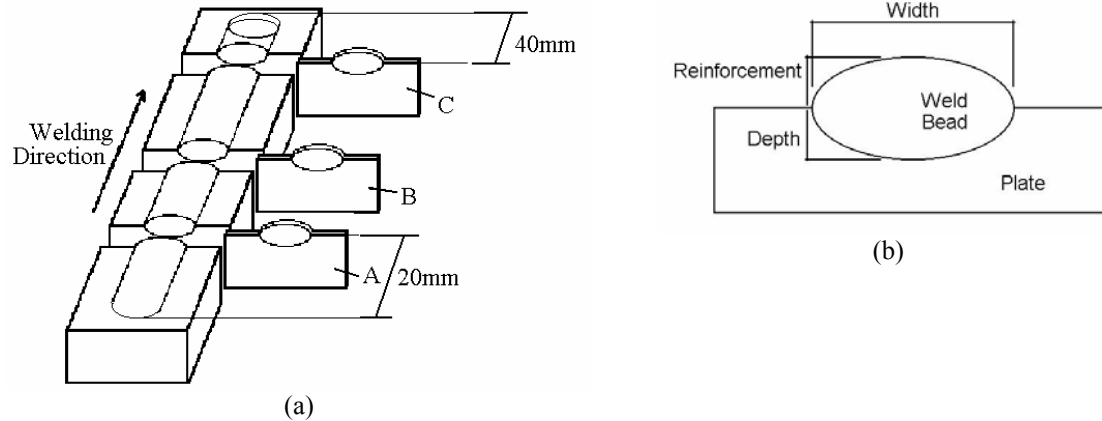


Figure 13. (a) Location of the transverse cross-section extracted from the bead-on-plate wet welds and (b) bead-on-plate weld showing the width, depth or penetration, and reinforcement.

### 3.2.1 On ASTM A36 steel

Figures 14 and 15 show photographs of the BOP wet welds deposited on A36 steel plates at 50 and 100 m. Additional photographs are included in Appendix B.



(a) E6013 with 260 A



(b) E7018 with 280 A



(c) E7024 with 310 A

Figure 14. Photographs of the bead-on-plate wet welds deposited with the three electrode types using electrode positive (DCEP) on A36 steel plates at 50 m.

Wider BOP welds were produced with the E7024 electrode type due to its thicker flux coating and flux content. This electrode type has iron powder in the flux to increase the

deposition rate. The BOP welds deposited with E7024 electrodes show better beads than those deposited with the E6013 and E7018 electrodes. More irregular beads (rough bead surface, variable width, and high reinforcement) were deposited with E6013 electrodes using DCEN.

Transverse cross-section macrographs from the center of the BOP wet welds deposited with the three electrodes using DCEP and DCEN at 50 and 100 m are included in Appendix C. Figure 15 presents cross-section macrographs from the BOP welds deposited with the three electrodes using DCEP on A36 steel plates at 50 m. In this case, E6013 produced the best cross-section, almost free of porosity.



(a) E6013 electrode at 50 m      (b) E7018 Electrode at 50 m      (c) E7024 electrode at 50 m

Figure 15. Cross-section macrographs from the center of the BOP wet welds deposited with the E6013, E7018 and E7024 electrodes using electrode positive (DCEP) at 50 m (scale in millimeters).

Bead morphologies were measured on three transverse cross-sections extracted from each BOP wet weld deposited with the three electrodes at two water depths on A36 steel plates, the measured values are given in Table 6.

Table 6. Averaged bead morphology values of the bead-on-plate wet welds deposited with the three electrodes at two water depths on A36 steel.

Electrode	Polarity	50 m			100 m		
		Width, mm	Penetration, mm	Reinforcement, mm	Width, mm	Penetration, mm	Reinforcement, mm
E6013	DCEP	12.7	1.3	2.9	13.5	2.2	3.2
E7018	DCEP	13.0	2.8	4.6	13.5	2.9	4.5
E7024	DCEP	18.9	2.7	4.2	20.1	2.0	4.4
E6013	DCEN	11.5	4.6	3.3	11.6	5.8	3.9
E7018	DCEN	14.1	4.0	4.3	13.8	3.8	4.4
E7024	DCEN	20.3	3.7	3.4	20.5	3.5	4.7

As one can see, there are large differences in the width of the BOP welds deposited with E6013 and E7018 electrodes with respect to those deposited with the E7024 electrodes. These differences are due to the differences in the flux coating thickness of the electrodes.

As mentioned above, the E7024 electrode has thicker flux coating (3 mm) with iron powder addition to increase the deposition rate. For this reason, this electrode type requires higher amperage than the other two electrode types, which resulted in the highest heat input of the BOP wet welds for both polarities (64 –81 kJ/in in DCEP and 71-95 kJ/in in DCEN). The penetration of the BOP wet welds also showed important differences. Deeper penetration was obtained with DCEN polarity than using DCEP, particularly with E6013 electrode type. The liquid metal dynamics in the weld pool could be the reason for the higher penetration obtained using DCEN. If the flow of the liquid metal in the weld pool is radially outward and into the steel plate, the penetration would be shallower and the weld bead wider. On the other hand, radially inward flow would result in deeper penetration and narrower weld beads, as clearly shown in Table 7 for the E6013 electrode type.

Table 7. Width and penetration measured on three cross-sections of the bead-on-plate wet weld deposited with E6013 electrode at 50 m and electrode negative.

<b>Cross-section</b>	<b>Width, mm</b>	<b>Depth, mm</b>
A	10.6	6,2
B	12.2	3,5
C	11.7	4,1

Compared with an average penetration value of 2 mm observed in the DCEP welds, the readings of 3.5, 4 and 6 mm represent increments between 175 and 300% in the DCEN welds.

Porosity measurements were carried out on the three cross-sections extracted from each BOP weld, the averaged results are given in Table 8. Also in this table are the percentages of porosity above baseline, which is defined as the percentage of pores located in the reinforcement area (topside) of the BOP welds. Pores located in the reinforcement area of a prior BOP welds could be remelted and removed with subsequent weld passes, resulting in a multipass weld with lower levels of porosity.

Table 8. Averaged porosity percentages measured on the cross-sections of the bead-on-plate wet welds deposited with the three electrodes at two water depths on A36 steel plates.

<b>Electrode type</b>	<b>Polarity</b>	<b>50 m</b>		<b>100 m</b>	
		<b>Porosity, %</b>	<b>Porosity % above baseline</b>	<b>Porosity, %</b>	<b>Porosity % above baseline</b>
E6013	DCEP	1.2	88	8.4	85
E7018	DCEP	17.8	71	20.2	72
E7024	DCEP	7.3	94	11.6	91
E6013	DCEN	9.8	29	14.9	31
E7018	DCEN	13.8	67	26.4	64
E7024	DCEN	5.4	73	22.8	81

From Table 8 the following comments can be made:

- a) E6013 electrodes produced the lowest levels of porosity (1.2% at 50m and 8.4 % at 100 m) using DCEP polarity.
- b) E7018 electrodes produced excessive porosity (17.8% at 50m and 20.2% at 100m) using DCEP, and the highest value (26.4%) using DCEN at 100m. Therefore, the E7018 electrode type is not suitable for underwater wet welding.
- c) Although E7024 electrodes produced more porosity than the E6013, large percentage of the pores is located above the baseline using DCEP, which could be removed in multipass welds.

In general, more porosity is produced using DCEN than DCEP polarity, with fewer pores located in the reinforcement area of the BOP welds. Therefore, DCEN should not be used in wet welding with the E6013 electrode type.

Micrographs taken on the cross-sections extracted from the center of the BOP welds deposited with the three electrodes on A36 steel at 50 m are shown in Figure 16. Additional micrographs are given in Appendix D.

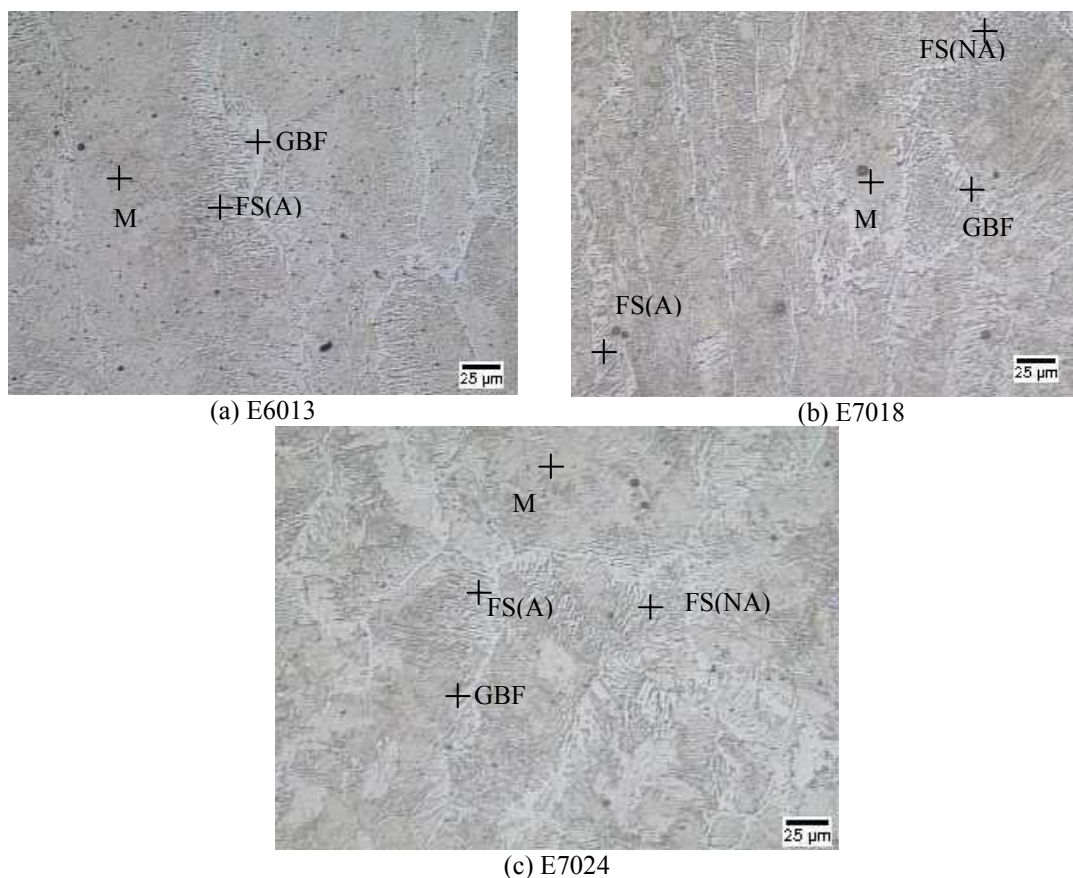
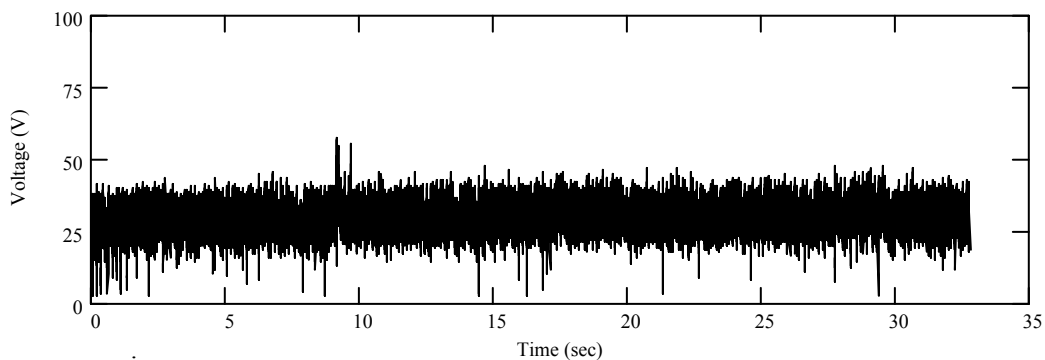


Figure 16. Microstructures of the bead-on-plate wet welds deposited with the three electrode types using electrode positive on A36 steel at 50 m.

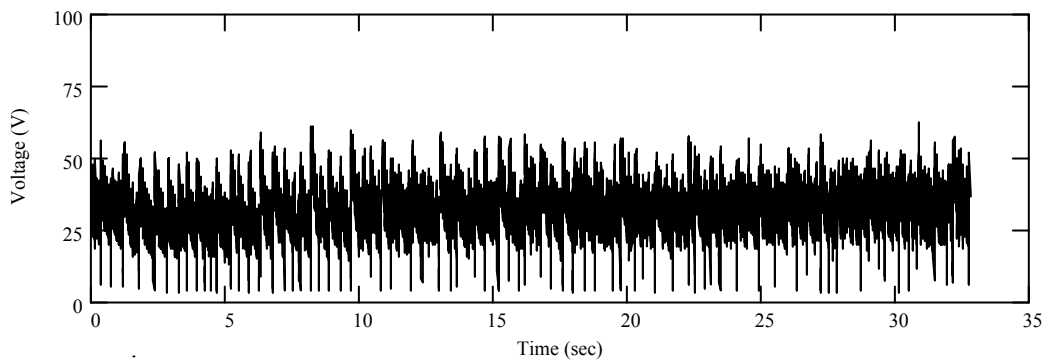
It is well established that in wet welding water breaks down into hydrogen and oxygen. Suga and Hasui (1986) determined that the main gas inside the pores in wet welds deposited with oxidizing electrodes was hydrogen (97%). Ibarra and Olson (1992) reported a rapid increase in the oxygen content of wet welds with increasing water depth, to a maximum content of about 0.19 % at approximately 40 ft. Oxygen content decreases slightly with further increasing water depth. Oxygen in the arc reacts with the liquid metal droplets leading to the oxidation of some of the alloying elements added to the electrode flux coating. These oxides may transfer to the slag or remain in the weld metal as inclusions. Due to the rapid increase of oxygen in the weld metal within the first 40 ft of water depth, a large percentage of the alloying elements in the steel rod or in the flux are lost due to oxidation. For this reason, large differences in the microstructure are not observed in the wet welds deposited at 50 and 100 m for any electrode-base steel combination.

Large percentages of acicular ferrite (AF) in weld metal microstructure generally indicate good mechanical properties. However, since wet welds are exposed to fast cooling rates it is difficult to form acicular ferrite. Typical microstructures observed in wet welds are ferrite with second phases aligned (FS(A)) and nonaligned (FS(NA)), grain boundary ferrite (GBF), martensite (M), and micro-constituents (MAC), see Figure 16.

The acquired arc voltage and current signals were analyzed. Figure 17 presents voltage signals acquired during wet welding with the three electrodes on A36 steel at 50 m. The entire analyzed signals and their corresponding spectra are provided in Appendix A.



(a) Globular with few short-circuiting indications



(b) Short-circuiting

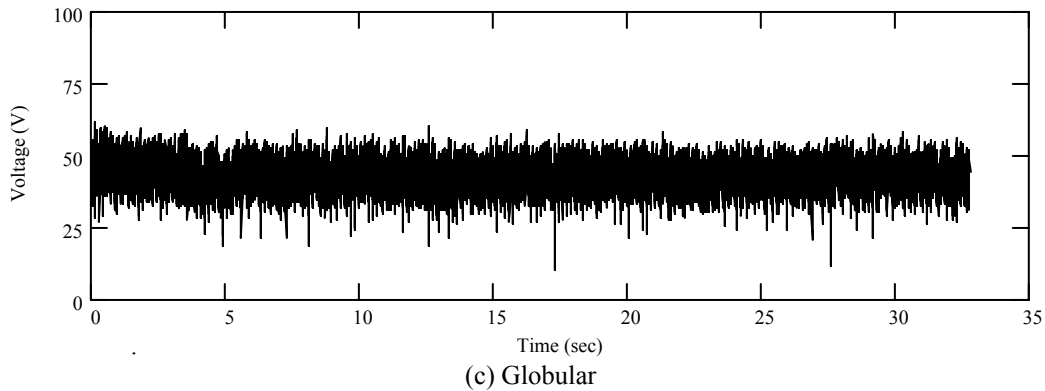


Figure 17. Voltage signals recorded during wet welding with (a) E6013 electrode, (b) E7018 electrode, and (c) E7024 electrode on A36 steel at 50 m water depth.

In Figure 17 one can easily determine the mean voltage values and the fluctuations around the mean value. The mean value is related to the arc length, which is the distance from the weld pool to the electrode tip or droplet attached to the tip of the electrode. On the other hand, the voltage fluctuations are related to the size of the droplets that form at the electrode tip. As the droplet size grows, the voltage decreases to a given value. After the droplet detaches from the electrode tip the voltage reaches a maximum value, and the cycle repeats. Similar voltage variations can be observed in the signals produced with the E6013 and E7024 electrodes, shown in Figure 17. The voltage signal generated with the E7018 electrode shows the largest fluctuations, reaching voltage values close to zero.

Metal transfer modes in the wet welding process as explained in Appendix A could be globular, short-circuiting or both. In short-circuiting mode, the droplets grow to a size equal to the arc length, touching the weld pool. The droplets then explode or transfer into the weld pool. This metal transfer mode was observed to occur when E7018 electrode was used, Figure 17 (b). Table 9 provides the metal transfer modes for each electrode type, polarity, and water depth.

Table 9. Metal transfer modes in wet welds deposited on A36 steel.

Steel plate	Electrode-polarity	At 50 m		At 100 m	
		Metal transfer modes	Metal transfer frequency (Hz)	Metal transfer modes	Metal transfer frequency (Hz)
A36	E6013-DCEP	G	0-10	G and SC	0-21
	E7018-DCEP	SC	0-5	SC	0-15
	E7024-DCEP	G	0-9	G	0-5
	E6013-DCEN	SC	0-20	SC	0-15
	E7018-DCEN	SC and G	0-3	SC	2.5
	E7024-DCEN	G	0-3	G	0-5

Note: G stands for globular and SC stands for short-circuiting

Metal transfer frequency refers to the frequency at which droplets transfer from the electrode tip to the weld pool. A wide range of frequencies could imply that the droplets have also a wide range of sizes. In Figure 17 (b), one can see large voltage drops (short-circuiting) at approximately 25 counts in the first 10 seconds. This behavior would result in a peak at approximately 2.5 Hz in the frequency domain or spectrum (when data is processed using the Fast Fourier Transform technique). The remaining signal would result in other peaks (transfer events) at different frequencies. The E6013 electrode exhibited globular metal transfer mode with DCEP at both water depths and short-circuiting with DCEN also at both water depths, the E7018 presented short-circuiting at all conditions, and the E7024 electrode showed globular transfer mode in all conditions.

From the acquired arc signals, mean values of the voltage, current, welding speed, and heat input were calculated and reported in Table 10.

Table 10. Mean voltage, current, welding speed, and heat input values calculated from the acquired arc signals from the BOP wet welds deposited on A36 steel.

BOP Weld	Polarity	Steel	Electrode	Water Depth, m	Selected Current, A	Avg. Current, A	Avg. Voltage, V	Welding Speed in/min	Heat Input kJ/in
11111	DCEP	A36	E6013	50	260	263	28.6	11.2	40.5
12112	DCEP	A36	E7018	50	280	284	31.4	11.5	46.6
13111	DCEP	A36	E7024	50	310	313	43.8	12.7	65.0
11211	DCEP	A36	E6013	100	280	285	30.6	12.2	43.2
12212	DCEP	A36	E7018	100	280	285	29.9	12.6	40.7
13211	DCEP	A36	E7024	100	310	280	50.8	10.9	78.2
11113	DCEN	A36	E6013	50	260	265	24.2	8.6	44.6
12114	DCEN	A36	E7018	50	280	282	33.2	9.8	57.3
13113	DCEN	A36	E7024	50	310	253	53.1	8.5	94.7
11213	DCEN	A36	E6013	100	280	285	27.8	10.6	45.0
12213	DCEN	A36	E7018	100	280	286	30	10.4	49.7
13213	DCEN	A36	E7024	100	310	294	45.9	11.0	73.5

From Table 10, the largest voltage value using DCEP polarity was 50.8 V and with DCEN was 53.1 V for the E7024 electrode at 100 and 50 m, respectively. These high values imply large arc lengths, in agreement with the fact that this electrode type has the thickest flux coating. The smallest voltage value, 24.2 V, corresponded to E6013 electrode with DCEN, which has the thinnest flux coating. Also in agreement with the discussion above are the heat input values. With the highest arc voltages, E7024 electrode type also resulted in the highest heat input, 94.7 kJ/in. Correspondingly, E6013 electrode type had the lowest heat input, 40.5 kJ/in.

The arc voltage signals acquired during wet welding with the three electrodes on A36 steel at 50 m and their corresponding spectra (power vs. frequency) are provided in Appendix A.

### 3.2.2 On ASTM A572 Gr. 50 steel

Photographs of the BOP wet welds deposited with the three electrodes using DCEP on A572 Gr. 50 steel plates at 50 and 100 m are included in Appendix B. Better weld beads were produced at 50 m than at 100 m. Also, wider BOP welds were produced with the E7024 electrode type due to its thicker flux coating and flux content. More irregular beads (surface roughness, variable width, and high reinforcement) were deposited with E6013 electrodes using DCEN. Many of the findings will parallel those for A36 steel welds.

The transverse cross-section macrographs from the center of the BOP wet welds deposited with the three electrode types using DCEP and DCEN polarity at 50 and 100 m are presented in Appendix C. From these macrographs, bead morphologies and porosity was characterized.

Bead morphologies from each BOP wet weld deposited with the three electrodes at two water depths on A572 Gr. 50 steel plates are given in Table 11.

Table 11. Averaged bead morphology values of the bead-on-plate wet welds deposited with the three electrodes at two water depths on A572 Gr. 50 steel.

Electrode	Polarity	50 m			100 m		
		Width, mm	Penetration, mm	Reinforcement, mm	Width, mm	Penetration, mm	Reinforcement, mm
E6013	DCEP	12.3	1.8	2.6	14.9	2.0	3.2
E7018	DCEP	11.8	3.0	4.0	13.4	3.0	4.8
E7024	DCEP	17.1	2.5	4.3	16.6	2.0	4.3
E6013	DCEN	11.2	3.3	2.6	12.4	3.8	4.4
E7018	DCEN	13.4	4.5	3.6	14.6	3.6	3.0
E7024	DCEN	20.3	3.5	4.0	19.7	3.2	4.2

There are no large differences with respect to the values obtained from BOP welds deposited on the A36 steel. Wider BOP welds were obtained with E7024 electrode using DCEN than with DCEP. Deeper BOP welds were produced with DCEN polarity, particularly with E6013 electrodes.

In general, BOP wet welds deposited with E6013 exhibited less porosity than with the other two electrodes, as can be seen in figures provided in Appendix C. Although the E7024 showed more porosity than the E7018 electrode type most of the pores are located close to the surface of the bop weld, in multipass welds these pores could be removed with the subsequent weld passes.

Porosity measurements were performed on the three cross-sections illustrated in Figure 13 (a). Table 12 shows the percentages of porosity with respect to the weld bead, and above baseline (in the reinforcement area) of the BOP welds.

Table 12. Averaged porosity percentages measured on the cross-sections of the bead-on-plate wet welds deposited with the three electrodes at two water depths on A572 Gr. 50 steel plates.

Electrode type	Polarity	50 m		100 m	
		Porosity, %	Porosity % above baseline	Porosity, %	Porosity % above baseline
E6013	DCEP	1.8	77.0	6.4	86.4
E7018	DCEP	10.1	40.6	18.0	60.4
E7024	DCEP	6.2	94.3	10.9	92.7
E6013	DCEN	5.0	34.1	13.4	43.5
E7018	DCEN	5.7	55.3	10.6	55.5
E7024	DCEN	5.6	92.8	10.1	80.5

From Table 12 the following comments can be made:

- a) E6013 electrodes produce the lowest levels of porosity (1.8% at 50 m and 6.4% at 100 m) at both water depths using DCEP polarity.
- b) E7018 electrodes produced the largest porosity percentages with both polarities (10.1 % at 50 m and 18.0 at 100 m with DCEP), but less porosity than that measured on BOP weld deposited on A36 steel.
- c) Although E7024 electrodes produced more porosity than the E6013, large percentage of the pores is located above the baseline.
- d) More porosity was produced with E6013 using DCEN than DCEP polarity at both depths.
- e) Welds deposited with E7018 and E7024 electrodes types presented more porosity when using DCEP than DCEN polarity at 50 and 100 m.
- f) More pores are located in the reinforcement area of the BOP welds deposited with E6013 using DCEP than when using DCEN polarity.
- g) In general, less porosity was measured in the BOP welds deposited on A572 Gr. 50 steel as compared with those deposited on the A36 steel.

Micrographs from the cross-sections extracted from the center of the BOP welds deposited with the three electrodes using DCEP at 50 and 100 m are included in Appendix D.

The acquired arc voltage and current signals were analyzed. The entire analyzed signals and their corresponding spectra are provided in Appendix A. Table 13 presents the metals transfer modes obtained from the acquired arc voltages signals. The metal transfer modes observed are similar to the ones obtained from the A36 steel and discussed in an earlier section.

Table 13. Metal transfer modes in wet welds deposited on A572 Gr. 50 steel.

Steel plate	Electrode-polarity	At 50 m		At 100 m	
		Metal transfer modes	Metal transfer frequency (Hz)	Metal transfer modes	Metal transfer frequency (Hz)
A572 Gr. 50	E6013-DCEP	G	0-7	G and SC	0-20
	E7018-DCEP	SC and G	0-6	SC	0-10
	E7024-DCEP	G	0-3	G	0-5 & 11-15
	E6013-DCEN	SC	4	SC	0-20
	E7018-DCEN	SC and G	0-7	SC	0-11
	E7024-DCEN	G	0-3	G	0-7

Note: G stands for globular and SC stands for short-circuiting

The E6013 electrode exhibited predominately globular metal transfer mode with DCEP at both water depths and short-circuiting with DCEN also at both water depths. The E7018 presented mainly short-circuiting mode at all conditions, and the E7024 electrode showed globular transfer mode in all conditions.

From the acquired arc signals, mean values of the voltage, current, welding speed, and heat input were calculated and reported in Table 14.

Table 14. Mean voltage, current, welding speed, and heat input values calculated from the acquired arc signals from the BOP wet welds deposited on A572 Gr. 50 steel.

BOP Weld	Polarity	Steel	Electrode	Water Depth, m	Selected Current, A	Avg. Current, A	Avg. Voltage, V	Welding Speed in/min	Heat Input kJ/in
21111	DCEP	A572-Gr.50	E6013	50	260	261	32.4	11.6	44.0
22113	DCEP	A572-Gr.50	E7018	50	280	278	36.0	11.6	51.7
23111	DCEP	A572-Gr.50	E7024	50	310	217	57.9	9.3	80.7
21211	DCEP	A572-Gr.50	E6013	100	280	285	28.4	12.1	40.2
22212	DCEP	A572-Gr.50	E7018	100	280	253	30.6	12.0	38.8
23211	DCEP	A572-Gr.50	E7024	100	310	203	59.0	9.0	80.3
21113	DCEN	A572-Gr.50	E6013	50	260	274	19.2	7.5	41.8
22114	DCEN	A572-Gr.50	E7018	50	280	282	33.4	9.2	62.0
23112	DCEN	A572-Gr.50	E7024	50	310	251	54.7	8.7	94.4
21213	DCEN	A572-Gr.50	E6013	100	280	289	25.9	9.1	49.4
22213	DCEN	A572-Gr.50	E7018	100	280	262	34.8	10.5	52.2
23213	DCEN	A572-Gr.50	E7024	100	310	271	49.3	8.4	95.1

From Table 14, the largest voltage value using DCEP polarity was 59 V and with DCEN was 54.7 V, both for the E7024 electrode at 100 and 50 m, respectively. These high values imply long arc lengths, again in agreement with the fact that this electrode type has the thickest flux coating. The smallest voltage value was 19.2 V and corresponded to the E6013 electrode with DCEN, which has the thinnest flux coating. Also in agreement with the discussion above are the heat input values. The largest value was 95.1 kJ/in, which

corresponded to E7024 electrode type and the smallest value was 38.8 kJ/in for the E7018 electrode type. The mean current value for the E7024 electrode using DCEP at 100 m was 203 A, which is considerably less than the pre-selected value of 310 A. This drop in the welding current values is associated with large fluctuations in the current signal in the time domain and also with large mean voltage value.

### 3.2.3 On API 5L Gr. B steel

Photographs of the BOP wet welds deposited on API 5L Gr. B steel plates at 50 and 100 m are provided in Appendix B. Again; wider BOP welds were produced with the E7024 electrode type due to its thicker flux coating and flux content. The BOP welds deposited with E7024 electrodes show better beads than those deposited with the E6013 and E7018 electrodes. More irregular beads (surface roughness, variable width, and high reinforcement) were deposited with E6013 electrodes using DCEN. The base metal composition difference (from the other two base metals) through dilution modifies the weld pool composition, thus affecting the weld bead formation.

The transverse cross-sections macrographs from the center of the BOP wet welds deposited using DCEP at 50 and 100 m are presented in Appendix C.

The bead morphologies were measured on the three transverse cross-sections extracted from each BOP wet weld deposited with the three electrodes at two water depths on API 5L Gr. B steel plates and the results are given in Table 15.

Table 15. Averaged bead morphology values of the bead-on-plate wet welds deposited with the three electrodes at two water depths on API 5L GR. B steel.

Electrode	Polarity	50 m			100 m		
		Width, mm	Penetration, mm	Reinforcement, mm	Width, mm	Penetration, mm	Reinforcement, mm
E6013	DCEP	13.1	1.7	2.9	15.6	2.1	3.3
E7018	DCEP	12.1	2.7	4.2	13.6	3.0	4.5
E7024	DCEP	18.6	2.5	4.3	17.6	2.6	4.1
E6013	DCEN	11.2	4.5	3.3	11.3	4.5	3.4
E7018	DCEN	13.3	4.6	4.5	14.7	3.6	4.5
E7024	DCEN	20.2	2.7	4.0	19.1	2.8	4.3

As mentioned earlier, this steel presented a carbon equivalent value of 0.41, which according to the experience may present some difficulties in wet welding. Cross-section macrographs showed hydrogen cracking in the heat-affected zone just under the fusion line. This problem is associated to the slightly harder steel due to the differences in chemical composition (larger manganese content in this case), cooling rate, and residual stress.

There were not large differences with respect to the bead morphology values obtained from BOP welds deposited on the other two steels. Wet welds deposited with E6013 electrodes using DCEN exhibited more penetration with respect to DCEP polarity. The high

reinforcement values of the welds deposited with E7018 could be due to the larger amount of entrapped gases in the weld metal.

Less porosity was observed in the BOP welds deposited with E6013 electrodes than those made with the E7018 and E7024 electrode type, see figures in Appendix C. The largest amount of pores was observed on the welds deposited with E7018 electrode type. Porosity measurements were carried out on the three cross-sections illustrated in Figure 13 (a) and the averaged results are given in Table 16. Also in this table are shown percentages of porosity above baseline of the BOP welds.

Table 16. Averaged porosity percentages measured on the cross-section of the bead-on-plate wet welds deposited with the three electrodes at two water depths on API 5L Gr. B steel plates.

Electrode type	Polarity	50 m		100 m	
		Porosity, %	Porosity % above baseline	Porosity, %	Porosity % above baseline
E6013	DCEP	0.6	71	8.8	78
E7018	DCEP	8.8	63	25.8	84
E7024	DCEP	8.3	88	13.4	79
E6013	DCEN	8.3	26	16.6	33
E7018	DCEN	14.8	42	24.4	76
E7024	DCEN	3.5	81	17.8	86

From Table 16 the following comments can be made:

- a) E6013 electrodes produce the lowest levels of porosity (0.6% at 50 m and 8.8 % at 100 m) using DCEP polarity.
- b) E7018 electrodes produced the largest percentage of porosity at both water depths and both polarities, very large percentages (25.8 % with DCEP and 24.4% with DCEN) were measured at 100 m.
- c) E7024 electrodes produced more porosity than the E6013, but less than the E7018 electrodes, large percentage of the pores are located above the baseline.
- d) More porosity is produced using DCEN than DCEP polarity, except E7024 electrode with DCEN at 50 m that exhibited a small percentage of porosity (3.5 %) and E7018 electrode with DCEN at 100 m that presented slightly less (24.4 %) porosity than DCEP.

Micrographs from the cross-sections extracted from the center of the BOP welds deposited with the three electrodes using DCEP at 50 and 100 m are included in Appendix D.

The metals transfer modes from the arc signals acquired during wet welding with the three electrodes, two polarities, and two water depths are summarized in Table 17.

Table 17. Metal transfer modes in wet welds deposited on API 5L Gr. B steel.

Steel plate	Electrode	At 50 m		At 100 m	
		Metal transfer modes	Metal transfer frequency (Hz)	Metal transfer modes	Metal transfer frequency (Hz)
API 5L Gr. B	E6013	SC and G	0-20	SC and G	0-21
	E7018	SC and G	0-3	SC	0-5
	E7024	G	0-3	G	2.5
	E6013	SC	2-18	SC	10-16
	E7018	SC	2.5	SC	2.5
	E7024	G	0-11	G and SC	0-8

Note: G stands for globular and SC stands for short-circuiting

The E6013 electrode exhibited short-circuiting and globular metal transfer modes with DCEP at both water depths and short-circuiting with DCEN also at both water depths. The E7018 electrode presented short-circuiting and the E7024 electrode showed globular transfer mode, under all conditions. The E6013 electrode with DCEP polarity switched from pure globular in the other two steels to pure short-circuiting in the API 5L Gr. B steel.

From the acquired arc signals, mean values of the voltage, current, welding speed, and heat input were calculated and reported in Table 18.

Table 18. Mean voltage, current, welding speed, and heat input values calculated from the acquired arc signals from the BOP wet welds deposited on API 5L Gr. B steel.

BOP Weld	Polarity	Steel	Electrode	Water Depth, m	Selected Current, A	Avg. Current, A	Avg. Voltage, V	Welding Speed in/min	Heat Input kJ/in
31111	DCEP	API 5L Gr. B	E6013	50	260	265	25.9	10.5	39.0
32112	DCEP	API 5L Gr. B	E7018	50	280	286	34.4	11.7	50.3
33111	DCEP	API 5L Gr. B	E7024	50	310	195	60.2	8.7	81.0
31211	DCEP	API 5L Gr. B	E6013	100	280	284	27.3	12.1	38.4
32211	DCEP	API 5L Gr. B	E7018	100	280	284	30.5	12.1	42.9
33211	DCEP	API 5L Gr. B	E7024	100	310	186	60.3	9.1	73.7
31113	DCEN	API 5L Gr. B	E6013	50	260	246	22.9	8.0	42.1
32113	DCEN	API 5L Gr. B	E7018	50	280	285	30.1	10.0	51.4
33113	DCEN	API 5L Gr. B	E7024	50	310	266	49.4	9.5	82.8
31213	DCEN	API 5L Gr. B	E6013	100	280	265	25.7	9.1	44.8
32213	DCEN	API 5L Gr. B	E7018	100	280	286	32.3	16.7	33.2
33213	DCEN	API 5L Gr. B	E7024	100	310	278	42.4	10.0	71.1

From Table 18, the largest voltage value using DCEP polarity was 60.3 V and with DCEN was 49.4 V for the E7024 electrode at 100 and 50 m, respectively. Again, these high values imply large arc lengths, which are in agreement with the fact that this electrode type has the

thickest flux coating. The smallest voltage value was 22.9 V and corresponded to the E6013 electrode with DCEN, which has the thinnest flux coating. Also in agreement with the above mentioned are the heat input values. The highest heat input value was 82.8 kJ/in for the E7024 electrode type and the smallest value was 33.2 kJ/in for the E7018 electrode type. The mean current value for the E7024 electrode using DCEP at 100 m was 186 A, which is considerably less than the selected value of 310 A. This drop in the welding current values is associated with large fluctuations in the current signal in the time domain and also with large mean voltage value.

### 3.3 Multipass V-groove wet welds

Twelve V-groove wet welds were deposited with two electrode types on three steels using DCEP at two water depths. Based on the arc extinctions observed during BOP welding and porosity results obtained with the E7018 electrode type, it was determined inappropriate to make V-groove wet welds. DCEN polarity was not used to deposit V-groove wet welds. Figure 4 illustrates the dimensions and arrangement of the plates used to make the V-groove wet welds. Welding current values given in Table 3 were used for each electrode and water depth. The plate-electrode angle was fixed at 60 degrees.

Figure 18 shows a picture of A572 Gr. 50 steel plates ready for V-groove wet welding and Figure 19 shows the same plates inside the chamber after depositing a wet weld bead.



Figure 18. Steel plate arrangement for V-groove welding.



Figure 19. V-groove wet weld inside the chamber after depositing another wet weld.

Considering that these welds were deposited in the V-groove formed by two plates where the starting point was approximately the same and the end point was different for each electrode, the end part of the V-groove was not completely filled in some cases.

### 3.3.1 On A36 steel

Photographs of the V-groove wet welds deposited with the E6013 and E7024 electrode types on A36 at 50 and 100 m are provided in Appendix E. X-ray radiographs of the V-groove wet welds are also included in Appendix E.

Although the V-groove weld deposited with E6013 electrode at 50 m shows some superficial defects, in general the weld beads have good appearance. Rougher weld surface is observed in the weld deposited at 100m. At 100 m, the amount of gases in the arc is larger due to the increase in pressure, and the bubbles exiting the weld surface just before the solidification of the weld metal leave behind these small holes.

In the X-ray radiograph of the weld deposited with E6013 electrode at 50 m a uniform distribution of pores is observed along the weld, larger pores are observed at the beginning part. Small differences are observed in the X-ray radiograph of the weld deposited at 100 m.

In the V-groove welds deposited with E7024 electrode at 50 and 100 m, rougher weld beads are observed. Small gaps are also observed in between weld passes that could result in slag entrapment or lack of fusion with the subsequent passes.

A large amount of pores is observed in the welds deposited with E7024 electrode at both water depths. Larger pores are also observed at the beginning part of the weld as compared with the welds deposited with E6013 electrodes.

### **3.3.2 On A572 Gr. 50 steel**

Photographs of the V-groove wet welds deposited with the E6013 and E7024 electrode types on A572 Gr. 50 steel at 50 and 100 m are provided in Appendix E. X-ray radiographs of the V-groove wet welds are also shown in Appendix E.

In general, the weld beads made with the E6013 electrode have good appearance. Rougher weld surface is observed in the weld deposited at 100m. The X-ray radiograph of the weld at 50 m shows a uniform distribution of fine pores along the weld; larger pores are observed in the beginning part. Larger pores are observed in the radiograph of the weld deposited at 100 m with respect to the V-groove weld deposited on A36 steel.

In the V-groove welds deposited with E7024 electrode at 50 and 100 m, rougher weld beads are observed. Again, small gaps are observed in between passes that could result in slag entrapment or lack of fusion when depositing subsequent passes.

More porosity is observed at the beginning of the welds deposited with E7024 electrode at both water depths than in the welds deposited with E6013 electrodes. Also larger pores are observed at the beginning part of the weld as compared with the welds deposited with E6013 electrodes.

### **3.3.3 On API 5L Gr. B steel**

Photographs of the V-groove wet welds deposited with the E6013 and E7024 electrode types on API 5L Gr. B steel at 50 and 100 m are provided in Appendix E. X-ray radiographs of the V-groove wet welds are also collected in Appendix E.

In general, the weld beads made with the E6013 electrode have good appearance. Rougher weld surface is observed in the weld deposited at 100m. In the X-ray radiograph of the weld deposited with E6013 electrode at 50 m, a uniform distribution of fine pores is observed along the weld, while larger pores are observed more in the beginning part. Also, larger pores are observed in the weld deposited at 100 m with respect to the V-groove weld deposited at 50 m.

In the V-groove welds deposited with E7024 electrode at 50 and 100 m, rougher weld beads are observed. Small gaps are observed in between passes that could result in slag entrapment or lack of fusion with the subsequent passes.

More porosity is observed in the welds deposited with E7024 electrode on API 5L Gr. B steel than in the welds deposited with E7024 electrodes on A572 Gr.50 and A36 steels at 50 m. Also larger pores are observed at the beginning part of the weld as compared with the welds deposited with E6013 electrodes.

### **3.3.4 Porosity of the V-groove wet welds**

Depending on how long the electrode is submerged in water and the pressure inside the chamber, the flux covering of the electrode could absorb water. Before placing the

electrode in the gravity welder, the waterproofing coating is peeled off from the tip of the electrode in order to have electrical conduction to start the arc. It is plausible that at exposure to water under pressure, one to two inches of the flux close to the peeled tip can absorb water, which then decomposes in the arc increasing the amount of gases absorbed in the liquid metal, thereby increasing porosity. Figure 20 shows the porosity on cross-section macrographs from V-groove wet welds. Figures 20 (a) and (c) correspond to the beginning part of the welds and Figures 20 (b) and (d) correspond to the end part. As shown, the percentage of porosity is larger at the beginning part of the multipass wet welds (wetted flux) than at the end part (dry flux). In agreement with the above discussion, Figure 21 presents a X-ray radiographic image taken from the V-groove wet weld deposited with E7024 electrodes on API 5L Gr. B steel at 100 m. Note the large amount of porosity at the beginning (left hand side) of the weld.

In actual repair works with wet welding, the wet welds are deposited by welder/divers who can remove the waterproofing coating from the tip of the electrode just before the arc starts. As such, this effect can be minimized. As to the weld results presented in this report, in particular microstructure and mechanical properties, this effect is of little concern since the beginning part of the V-groove welds was discarded.



(a) E6013 at 50 m, 5.2 %



(b) E6013 at 50 m, 2.1%



(c) E7024 at 100 m, 22.8%



(d) E7024 at 100 m, 8.4%

Figure 20. Cross-sections macrographs extracted (a) and (c) from the beginning and (b) and (d) from the end part of the V-groove welds. All four macrographs are shown at the same magnification.

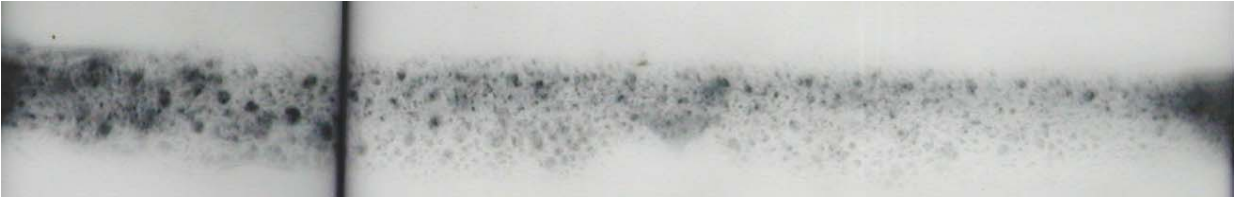


Figure 21. X-ray radiographic image from the V-groove wet weld deposited with E7024 electrodes on API 5L Gr. B steel at 100 m. Larger pores are observed on the left hand side, which is the beginning of the weld.

Porosity percentages measured on V-groove wet welds deposited with E6013 electrodes at two water depths are shown in Figure 22.

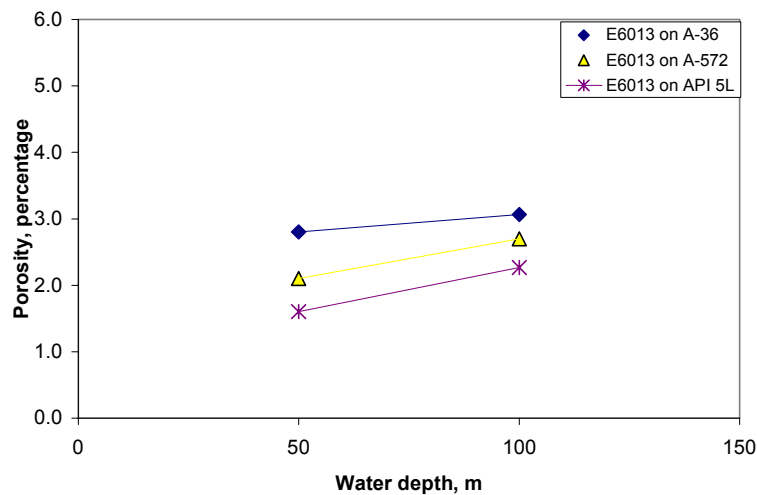


Figure 22. Porosity versus water depth from V-groove wet welds deposited with E6013 electrodes on three steels

It is easy to notice that porosity slightly increases with increasing water depth. Larger water depth effect was observed with the E7024 electrode, which at 100 m produces more than two times the porosity observed at 50 m, as shown in Figure 23.

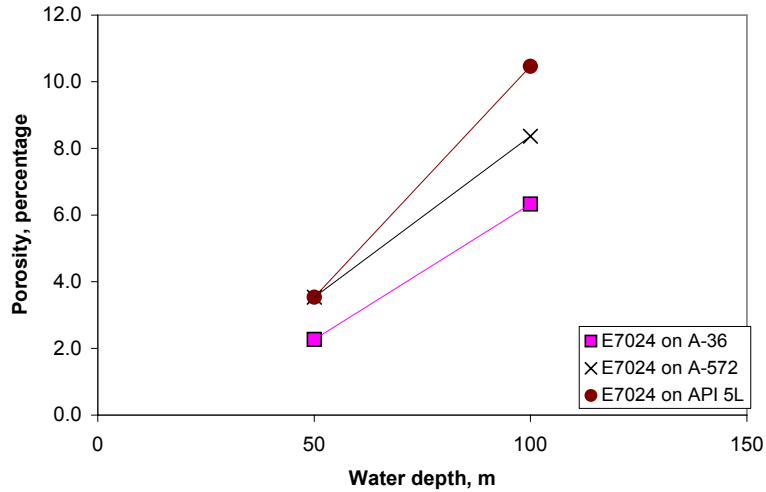


Figure 23. Porosity versus water depth from V-groove wet welds deposited with E7024 electrodes on three steels.

E7024 electrode type at 100 m produced 10.5% porosity on API 5L Gr. B steel, 8.4 % on A572 Gr. 50 steel and 6.3 % on A36 steel. As can be seen in Figure 24, the porosity produced with E7024 electrode at 100 m is significantly different from that produced with the E6013 electrode. However the porosity percentages at 50m are similar with the two electrodes. E6013 electrode exhibited very similar porosity percentages at the two water depths.

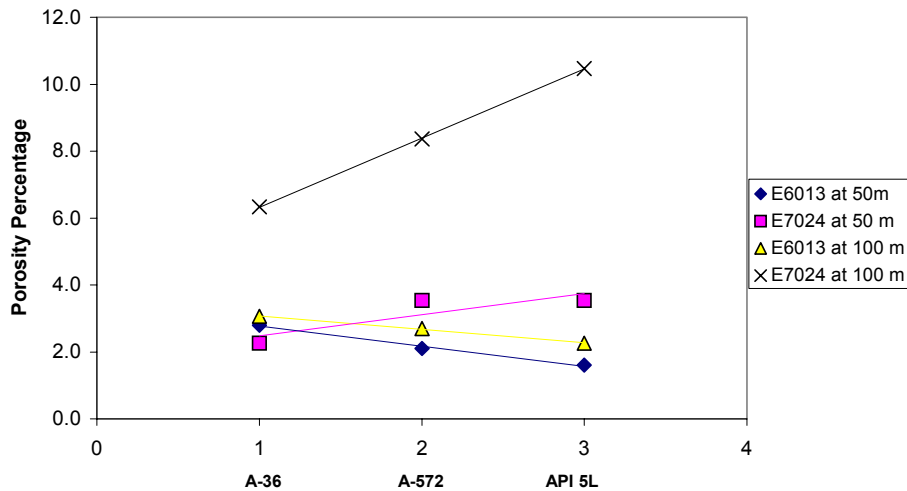


Figure 24. Porosity versus steel type from V-groove wet welds deposited with E7024 and E6013 electrodes at 50 and 100 m.

As above mentioned, the 7024 electrode type presented the largest arc length and widest beads. This implies that the arc volume is larger than with the E6013 electrode. With a large arc volume and increasing the water depth; the amount of moisture in the arc

increases resulting in larger amount of porosity. It is clearly shown in Figure 24 that the porosity percentages obtained with the AWS E6013 and E7024 electrode grade at 50 m are under 4%, which is smaller than the 6.0 - 8.5 % reported by Suga and Hasui, (1986) at the same depth.

### 3.4 Mechanical testing

#### 3.4.1 Tensile testing

Tensile testing was carried out on specimens illustrated in Figure 7. The results obtained from the welds deposited at 50 m are presented in Table 19 and the results from welds deposited at 100 m are given in Table 20, the tensile strength of the base metal is giving for reference. The ultimate tensile strength (UTS) of the welds made at 50 m reported values higher than the UTS of the base metal, and the welds deposited at 100 m reported values in the range from 42 to 59 ksi. The tensile strength of the welds deposited with E6013 electrodes at 100 m reported values close to the UTS of the base metal and the welds deposited with E7024 electrodes at 100 m reported values under the UTS of the base metal. These low values are the result of the porosity increase and alloying element loss with increasing water depth. Yield strength values were not calculated because the tensile specimens were extracted perpendicularly to the weld axis as illustrated in Figure 7. There were two different steels (base metal and welds metal) in the gauge length of the specimen.

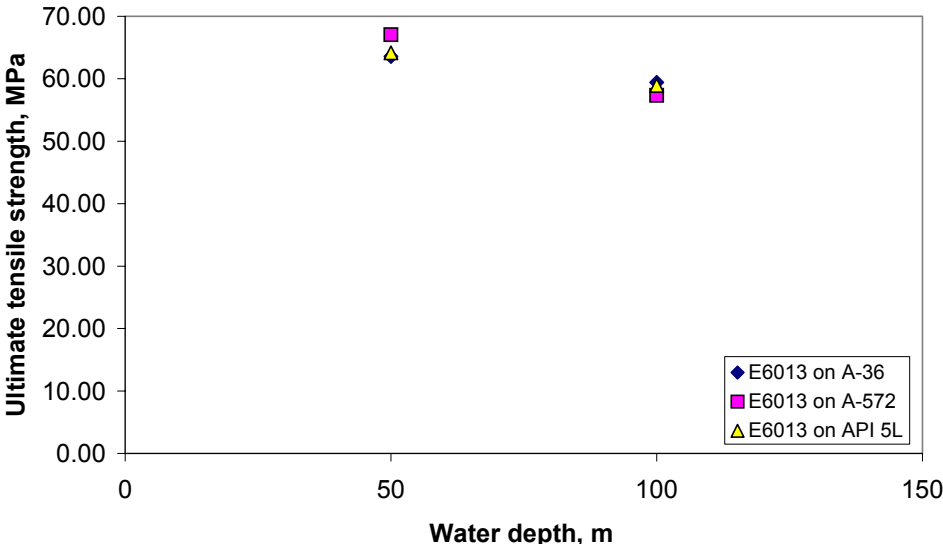
Table 19. Tensile test results of wet welds deposited at 50 m.

Electrode	Steel	Base metal (ksi)	Avg. (ksi)	Min. (ksi)	Max. (ksi)
E6013	A36	60	63.6	61.7	65.4
	A572 Gr. 50	65	67.1	66.3	67.8
	API 5L Gr. B	60	64.2	62.3	66.0
E7024	A36	60	62.7	58.5	66.9
	A572 Gr. 50	65	65.6	62.4	68.7
	API 5L Gr. B	60	63.1	59.8	66.4

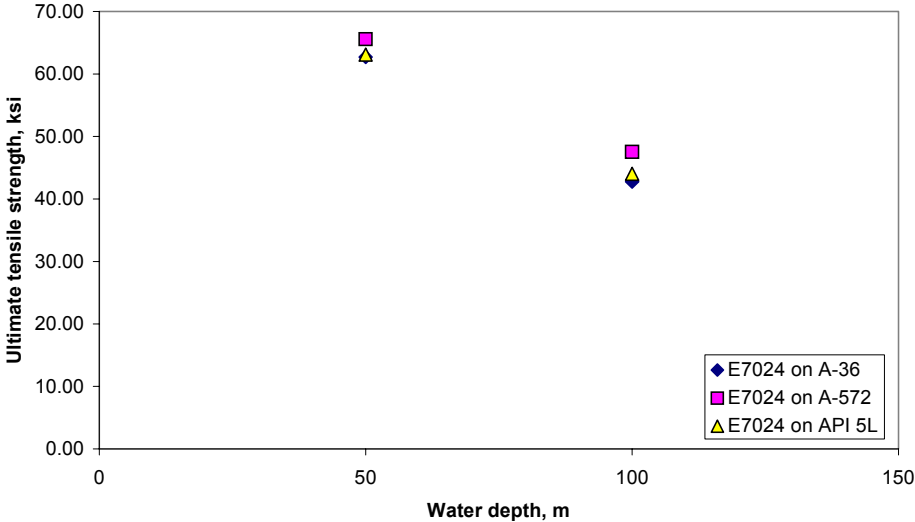
Table 20. Tensile test results of wet welds deposited at 100 m.

Electrode	Steel	Base metal (ksi)	Avg. (ksi)	Min. (ksi)	Max. (ksi)
E6013	A36	60	59.4	57.1	61.7
	A572 Gr. 50	65	57.4	55.4	59.3
	API 5L Gr. B	60	59.0	57.1	60.8
E7024	A36	60	42.8	38.2	47.4
	A572 Gr. 50	65	47.5	42.4	52.7
	API 5L Gr. B	60	44.0	43.0	45.1

Figure 25 shows the results presented in Tables 19 and 20. The averaged UTS value of wet welds deposited with E6013 electrode type at 100 m reported values 90% of the averaged value obtained from welds deposited with the same electrode type at 50 m. On the other hand, the wet welds made with E7024 electrode type at 100 m reported only 70% of the averaged values obtained in wet welds deposited at 50 m. The low UTS values obtained with E7024 electrode type at 100 m. are attributed to the larger percentages of porosity.



(a) Wet weld deposited with E6013 electrode type.



(b) Wet weld deposited with E7024 electrode type

Figure 25. Ultimate tensile strength of V-groove wet welds deposited with E6013 and E7024 electrode type at two water depths.

The tensile strength obtained (63-67 ksi) with the AWS E6013 and E7024 electrode grade at 50 m is comparable to that reported by Pope (1997) at 12 m (64 ksi) and 20 m (65 ksi) and by Grubbs (1998) at 50 m (66 ksi). At 100m, the tensile strength obtained with E6013 Electrode grade (60 ksi) was slightly under the results reported by Szelagowski (1990) (65 ksi).

### 3.4.2 Charpy impact testing

The reduced sized Charpy specimens were tested at 0 °C and the results are given in Tables 21 and 22 for the welds deposited at 50 m and 100 m, respectively. Figure 26 shows graphically the results. The difference of impact toughness values obtained is very small for the welds made with E6013 electrodes at 50 m.

Table 21. Charpy impact test results of wet welds deposited at 50 m.

Electrode	Steel	Avg. (ft-lbf)	Min. (ft-lbf)	Max. (ft-lbf)	Avg. * (ft-lbf)	Min. * (ft-lbf)
E6013	A36	18.9	17.6	20.2	15	10
	A572 Gr. 50	17.0	17.0	17.1		
	API 5L Gr. B	19.1	19.1	19.2		
E7024	A36	22.1	20.1	24.0		
	A572 Gr. 50	18.5	17.5	19.6		
	API 5L Gr. B	14.3	13.9	14.8		

\* Requirement for Class A wet welds according to AWS D3.6M:1999

Table 22. Charpy impact test results of wet welds deposited at 100 m.

Electrode	Steel	Avg. (ft-lbf)	Min. (ft-lbf)	Max. (ft-lbf)	Avg. * (ft-lbf)	Min. * (ft-lbf)
E6013	A36	14.8	13.6	16.0	15	10
	A572 Gr. 50	14.7	14.6	14.8		
	API 5L Gr. B	15.9	15.1	16.7		
E7024	A36	14.8	13.4	16.2		
	A572 Gr. 50	13.9	13.7	14.1		
	API 5L Gr. B	11.4	8.9	13.9		

\* Requirement for Class A wet welds according to AWS D3.6M:1999

Although the specimens were reduced size the toughness values reported at 50 m (with the exception of the E7024 and API 5L Gr. B steel) for the three steels exceed the average value required by the AWS D.6 M:1999 for Class A welds (welds for structural applications similar to above-water welds).

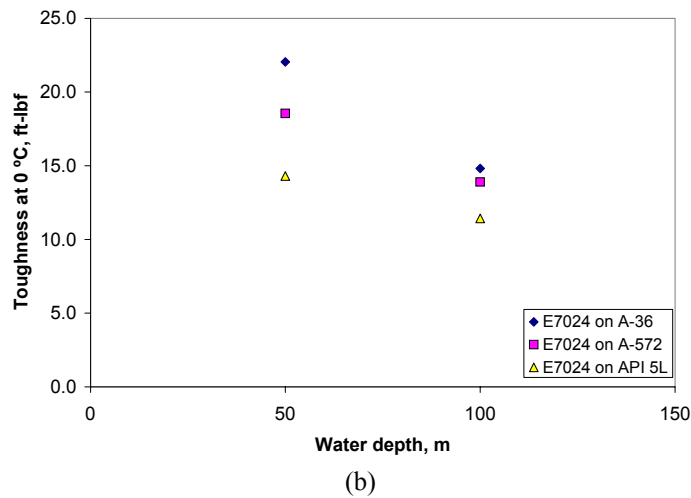
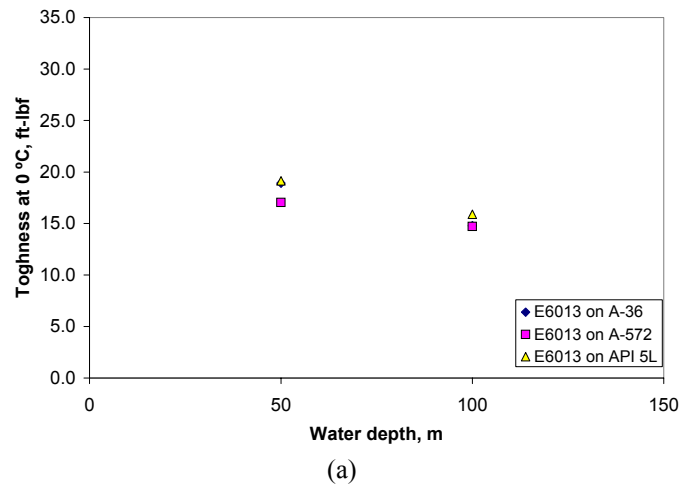


Figure 26. Charpy impact testing results of reduced size specimens machined from the V-groove wet welds, the tests were carried out at a temperature of 32 °F (0 °C).

The Charpy impact toughness results obtained with the AWS E6013 and E7024 electrode at 50 m (14-22 ft-lb) are comparable with results reported by Szelagowski at 55 m (18 ft-lb) using nickel as alloying element to improve toughness. The toughness results obtained at 100m with both electrodes (11-16 ft-lb) are comparable with the results reported by Szelagowski (1990) at same depth (12-18 ft-lb), also using nickel to improve toughness.

### 3.4.3 Bend testing

The average, minimum and maximum loading results from the side bend tests are given in Tables 23 and 24. The Average values are also shown in Figure 27. The wet welds deposited with the E6013 electrode supported higher bending loads than the welds made with E7024 electrode at both water depths (except on A36 steel at 50 m). From the E7024 welds at 50 and 100 m, it is clear that the maximum bending load decreased with increasing water depth, and that the A-36 steel presented better performance, followed by the A-572 Gr. 50. The API 5L Gr. B steel exhibited the lowest bending loads.

Table 23. Side bend test results of wet welds deposited at 50 m.

Electrode	Steel	Avg. (lbf)	Min. (lbf)	Max. (lbf)	Test Bend Radius	Max. Test bend radius *
E6013	A36	714	666	745	2.7 T	2 T
	A572 Gr. 50	871	827	917	> 3 T	
	API 5L Gr. B	809	785	825	2.2 T	
E7024	A36	697	569	855	2.0 T	
	A572 Gr. 50	716	604	860	2.0 T	
	API 5L Gr. B	620	593	661	1.4 T	

\* Requirement for Class A wet welds according to AWS D3.6M:1999, T is the specimen thickness

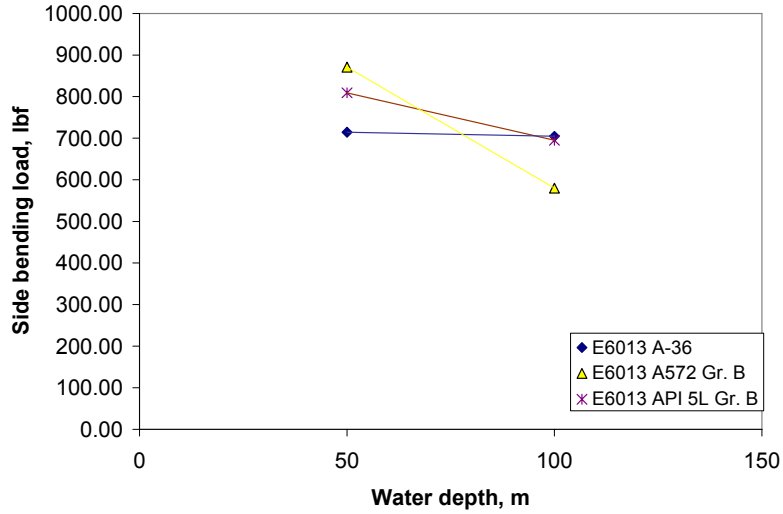
Table 24. Side bend test results of wet welds deposited at 100 m.

Electrode	Steel	Avg. (lbf)	Min. (lbf)	Max. (lbf)	Test Bend Radius	Max. Test bend radius *
E6013	A36	705	650	796	2.2 T	2 T
	A572 Gr. 50	580	503	620	1.9 T	
	API 5L Gr. B	695	670	723	2.0 T	
E7024	A36	512	419	626	1.3 T	
	A572 Gr. 50	445	355	503	0.8 T	
	API 5L Gr. B	398	328	487	0.6 T	

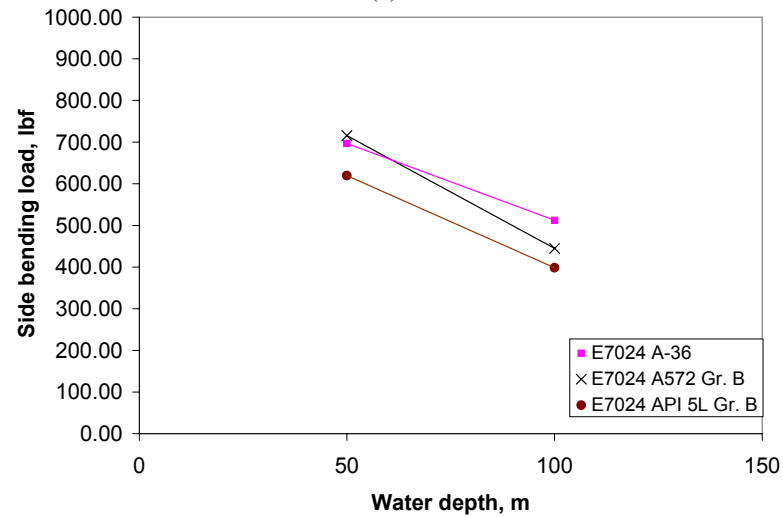
\* Requirement for Class A wet welds according to AWS D3.6M:1999, T is the specimen thickness.

With the exception of the weld deposited with E7024 electrode type on API 5L Gr. B steel at 50 m, all the other welds deposited at 50 m meet or exceed the AWS D3.6M:1999 2T requirement for Class A wet welds. Also, one could say that the welds deposited with E6013 electrodes at 100 m meet the 2T requirement. Wet welds deposited with E7024 at 100 m do not meet the 2T requirement.

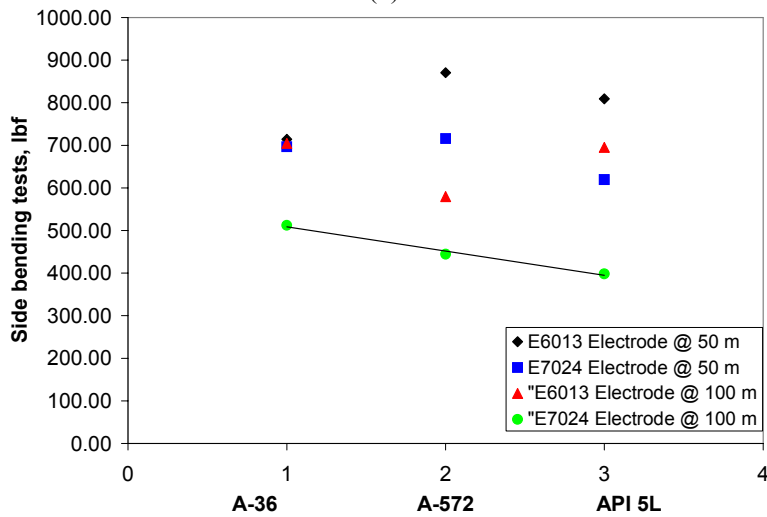
Figure 27 shows graphically the values in Tables 23 and 24. As can be seen, welds with electrode E6013 supported higher bending loads at both water depths



(a)



(b)



(c)

Figure 27. Results from the side bend test (a) specimens extracted from V-groove welds deposited with E6013 electrode and (b) with E7024 electrode.

## 4. CONCLUSIONS AND RECOMMENDATIONS

### 4.1 conclusions

An extensive amount of work has been carried out in this research program at least 85 BOP wet welds and more than 144 wet weld beads in the V-groove welds have been successfully deposited at simulated water depths of 50 and 100 m using the gravity welding system. One water depth (150 m) was not covered due to technical difficulties to deposit the wet welds. In general the wet welds deposited with the AWS E6013 electrode grade meet or exceed the AWS D3.6M:1999 requirements for Class A welds. The welds deposited with the AWS E7024 electrode grade at 50 m meet the AWS D3.6M:1999 requirements for Class A welds. Wet welding could also be an economic alternative to repair of floating production systems (FPSO's), for the repair of pipelines and other offshore structures.

Based on the results obtained from this project the main conclusions are:

1. It was possible to deposit BOP and V-groove wet welds at 50 and 100m water depths with the gravity welder inside the hyperbaric chamber.
2. The AWS E6013 electrode grade exhibited the best performance, less porosity and best mechanical properties, meeting or exceeding the AWS D3.6M:1999 requirements for Class A welds.
3. Under the conditions tested, i.e. mechanized, the AWS E7018 electrode grade presented poor performance, arc instability and large amount of pores making it unsuitable for wet welding.
4. Although the AWS E7024 electrode exhibited excellent performance with regards to its ability to start and maintain the arc, the amount of porosity that it produced was larger than that with the E6013 electrode grade, particularly at 100 m water depth.
5. Direct current electrode negative should not be used in mechanized wet welding applications with AWS E6013 electrodes, because of the larger amount of porosity obtained as compared with electrode positive polarity. However, the AWS E7024 electrode grade could be used with electrode negative polarity, which in some cases presented reduced porosity levels.
6. The porosity percentages obtained with the AWS E6013 and E7024 electrode grade at 50 m were under 4% which is smaller than the 6.0 - 8.5 % reported by Suga and Hasui, (1986) at the same depth.
7. The tensile strength obtained (63-67 ksi) with the AWS E6013 and E7024 electrode grades at 50 m are comparable to that reported by Pope (1997) at 12 m (64 ksi) and 20 m (65 ksi) and by Grubbs (1998) at 50 m (66 ksi). At 100m, the tensile strength

obtained with E6013 Electrode grade (60 ksi) was slightly under the results reported by Szlagowski (1990) (65 ksi).

8. The Charpy impact toughness results obtained with the AWS E6013 and E7024 electrode at 50 m (14-22 ft-lb) are comparable with results reported by Szlagowski at 55 m (18 ft-lb) using nickel as alloying element to improve toughness. The toughness results obtained at 100m with both electrodes (11-16 ft-lb) are comparable with the results reported by Szlagowski (1990) at same depth (12-18 ft-lb), also using nickel to improve toughness. Standard size Charpy V-notch specimens are expected to give higher toughness values than the ones reported.
9. Based on the mechanical properties of the welds deposited at 50 m the AWS E7024 electrode grade can be used at this depth. Care needs to be given to: a) the overlapping of the weld beads, b) minimize water absorption of the flux coating, and c) start each weld pass at different position to avoid concentration of pores.

## 4.2 Recommendations

The recommendations derived from this project are as follows:

1. Continue the experimental work with cellulosic electrodes at similar conditions. This electrode type gives more penetration and deposits a light slag that can easily be removed; minimizing time, weld defects, and costs. Therefore, multipass welds made with the cellulosic electrode grade could give fewer defects in the weld metal. With other electrode types such as E6013 electrode grade grinding to remove imperfections or slag entrapment of the wet welds is frequently necessary before placing the next weld bead. Although different electrode types have been tested in wet welding applications no data is available on the use of cellulosic electrodes.
2. New electrodes can be designed to improve the wet welds based on the experience obtained from this and previous research projects. Alloying elements such as manganese, silicon has been added to the flux coating to compensate the loss of these elements by oxidation. Sanchez-Osio (1993) and Rowe (1999) used titanium and boron additions to produced large percentages of acicular ferrite in the microstructure of wet welds; this microstructure is associated with good mechanical properties, particularly toughness improvements. The addition of titanium, boron, and manganese improve the tensile strength of wet welds, Rowe (1999). Pope (1995) and Perez (2003) demonstrated that nickel additions to the flux coating of oxidizing and rutile type electrodes, respectively improved toughness of wet welds deposited at 3.5 and 1 ft water depth.
3. The water absorption of the flux covering is an important issue that needs to be probed with additional experiments specifically designed for this purpose to verify the non-uniform distribution of pores along the length of the weld.
4. Since the main problems of wet welding are porosity and loss of alloying elements and that the loss of alloying elements can be compensated with over designing the

wet weld, it is important to conduct research work on minimizing the weld metal porosity. Thereafter it is necessary to determine the type of gases entrapped in the pores and its origin (moisture pickup, flux ingredients, etc.). Known the type of gases in the pores and their origin the chemical composition of the flux coating can be manipulated to minimize porosity.

5. In order to determine if the electrodes tested in this project are not suitable for wet welding at 150 m water depth more experimental wet welds need to be deposited varying the welding speed and heat input (by varying the welding current values and electrode-plate angles). If the electrodes were not appropriate for wet welding at 150 m additional welds would need to be deposited at shallower depths to determine the limiting water depth for this electrodes.
6. Safety and reliability issues are important in the different stages of offshore structures. There are many reasons to determine that aging structures may not meet requirements of current codes (damages, changes of service, addition of wells, well intervention, etc.) therefore underwater repairs or structural reinforcement may become necessary. Reliability of repair procedure needs to be known to properly determine the local and/or global reliability of the structure. For the above mentioned the reliability of wet welds deposited under specific conditions need to be determine.

## **5. ACKNOWLEDGMENTS**

The participants of this project acknowledge the support provided by the Minerals Management Service, in particular Dr. Charles Smith and Mr. Michael Else. The participants of this project wish to further acknowledge the support of the Instituto Mexicano del Petroleo.